ORIGINAL RESEARCH

Carotid Artery Echolucency, Texture Features, and Incident Cardiovascular Disease Events: The MESA Study

Carol C. Mitchell, PhD; Claudia E. Korcarz, DVM; Adam D. Gepner, MD; Rebecca Nye, BS; Rebekah L. Young, PhD; Mika Matsuzaki, PhD; Wendy S. Post, MD, MS; Joel D. Kaufman, MD, MPH; Robyn L. McClelland, PhD; James H. Stein, MD, FAHA

Background—We hypothesized that measures of common carotid artery echolucency and grayscale texture features were associated with cardiovascular disease (CVD) risk factors and could predict CVD events.

Methods and Results—Using a case-cohort design, we measured common carotid artery ultrasound images from 1788 participants in Exam 1 of the MESA study (Multi-Ethnic Study of Atherosclerosis) to derive 4 grayscale features: grayscale median, entropy, gray level difference statistic-contrast, and spatial gray level dependence matrices-angular second moment. CVD risk factor associations were determined by linear regression. Cox proportional hazard models with inverse selection probability weighting and adjustments for age, sex, race/ethnicity, CVD risk factors, and C-reactive protein were used to determine if standardized values for grayscale median, entropy, gray level difference statistic-contrast, and spatial gray level dependence matrices-angular second moment could predict incident coronary heart disease, stroke, and total CVD events over a median 13 years follow-up. Participants were mean (SD) 63.1 (10.3) years of age, 52.6% female, 32.1% white, 27.8% black, 23.3% Hispanic, and 16.8% Chinese. There were 283 coronary heart disease, 120 stroke, and 416 CVD events. Several associations of grayscale features with CVD risk factors were identified. In fully adjusted models, higher gray level difference statistic-contrast was associated with a lower risk of incident coronary heart disease (hazard ratio 0.82, 95% CI 0.71–0.94, p_{adj}=0.005) and CVD events (hazard ratio 0.87, 95% CI 0.77–0.98, p_{adj}=0.018); higher spatial gray level dependence matrices-angular second moment was associated with a higher risk of CVD events (hazard ratio 1.09, 95% CI 1.00–1.19, p_{adj}=0.044).

Conclusions—Gray level difference statistic-contrast and spatial gray level dependence matrices-angular second moment predicted CVD events independent of risk factors, indicating their potential use as biomarkers to assess future CVD risk. **(*J Am Heart Assoc*. 2019;8:e010875. DOI: 10.1161/JAHA.118.010875.)**

Key Words: cardiovascular events • carotid artery • texture features • ultrasound

B-mode grayscale ultrasound imaging traditionally is used to identify arterial injury, manifested as carotid artery atherosclerotic plaque or increased intima-media thickness (IMT), however advances in software and image analysis permit characterization of the arterial wall beyond macroscopic changes.[1–6] Advances in image analysis allow for the use of statistical analyses of grayscale pixel density, brightness, and variation, measures that have been used to characterize tissue composition in carotid plaques and more recently, the arterial wall.[6–17] First-order statistics derived from the image histogram, such as the grayscale median (GSM) and entropy, are used to characterize the overall echogenicity and randomness in a segmented region of interest of the arterial wall.[6,7,9,18] Statistical methods such as gray level difference statistics (GLDS) and spatial gray level dependence matrices (SGLDM) can describe spatial

From the Division of Cardiovascular Medicine, Department of Medicine, School of Medicine and Public Health, University of Wisconsin, Madison, WI (C.C.M., C.E.K., A.D.G., R.N., J.H.S.); Department of Medicine, Division of Cardiovascular Medicine, William S. Middleton Memorial Veterans Hospital, Madison, WI (A.D.G.); Department of Biostatistics (R.L.Y., M.M., R.L.M.), and Departments of Environmental & Occupational Health Sciences, Medicine, and Epidemiology (J.D.K.), University of Washington, Seattle, WA; Division of Cardiology, Department of Medicine, Johns Hopkins University, Baltimore, MD (W.S.P.).

Accompanying Data S1 and Figures S1 through S9 are available at https://www.ahajournals.org/doi/suppl/10.1161/JAHA.118.010875

The abstract for this work was presented as a poster presentation at the American Heart Association Scientific Sessions, November 10 to 12, 2018 in Chicago, IL.

Correspondence to: Carol Mitchell, PhD, University of Wisconsin, Division of Cardiovascular Medicine, Department of Medicine, University of Wisconsin School of Medicine and Public Health, K6/322 Clinical Science Center, 600 Highland Ave MC 3248, Madison, Wisconsin 53792. E-mail: ccm@medicine.wisc.edu

Received September 18, 2018; accepted November 27, 2018.

Clinical Perspective

What Is New?

- Measures that characterize ultrasound grayscale brightness (grayscale median) and texture (entropy, contrast, spatial gray level dependence) are associated with several cardiovascular disease risk factors and risk of cardiovascular disease events.

What Are the Clinical Implications?

- These measures of carotid arterial wall echogenicity and texture describe arterial wall structure, composition, and changes associated with early arterial injury and have potential to be used as imaging biomarkers to assess future risk of cardiovascular disease.

relationships between 2 pixels.[7,9,18] Previous studies have demonstrated variable associations of carotid artery GSM, entropy, gray level difference statistics-contrast (GLDS-C) and angular second moment (ASM) with cardiovascular disease (CVD) risk factors and events, however these studies were small,[19] had few outcome events,[2] and/or had inconsistent findings.[11,12,16,17,20] We hypothesized that novel measures of carotid artery echolucency and grayscale texture features were associated with traditional and non-traditional CVD risk factors and could predict incident CVD events in middle-aged adults.

Methods

The data are available to other researchers through the National Institutes of Health, National Heart, Lung, and Blood Institute, Biologic Specimen and Data Repository Information Coordinating Center.[21,22] Analytic methods (eg, R code) may be requested from the author as there is presently no public access mechanism for archival of individual manuscript coding files. Researchers with interest in the ultrasound images or other study materials are invited to contact MESA (Multi-Ethnic Study of Atherosclerosis) via the study authors about access to images which are held internally at MESA because of the size of the archive and to protect participant privacy in accordance with participant consent.

Participants

This study was approved by the institutional review boards at each field center, the University of Wisconsin Carotid Ultrasound Reading Center, and the University of Washington Data Coordinating Center. Each participant provided informed consent before participation.[21,23] Details on MESA have been previously published.[21] Briefly, the MESA is a National Heart, Lung, and Blood Institute (NHLBI)-funded longitudinal cohort study that is evaluating the prevalence, progression and CVD risk factor associations of correlates and progression of subclinical CVD in a multi-ethnic population. At the time of recruitment, participants were between the ages of 45 to 84 years and did not have known CVD.[21] We used a case-cohort study design[24–26] to study participants from the MESA that had a carotid ultrasound study at Exam 1 (2000–2002) performed at 4 field centers (Baltimore County and Baltimore City, Maryland; Chicago, Illinois; Los Angeles County, California; and New York, New York). Participants from 2 other field centers were not evaluated because their ultrasound images were acquired using a different grayscale map that altered the grayscale echolucency and texture features analyzed in this report. The Exam 1 population selected for this analysis consisted of all cases, defined as participants that had any CVD event (myocardial infarction, resuscitated cardiac arrest, definite angina followed by revascularization, stroke, stroke death, coronary heart disease [CHD], CHD death, other atherosclerotic death, other CVD death; n=491) adjudicated between 2000 and 2013 and a randomly selected subcohort (n=1559) from 4651 eligible participants, for a total of 2050 participants analyzed. Of note, some data from 151 participants were included in our pilot study.[17]

CVD Risk Factor Assessments

Questionnaires were given to participants to obtain data on demographics, smoking history, family history of CVD, alcohol consumption, medical history, prescription medications, non-prescription medications, dietary intake, psychosocial parameters, and physical activity.[21] Anthropomorphic measurements of weight and height were recorded.[21,23,27] Seated blood pressures were measured in triplicate with the mean of the last 2 used for analysis (Dinamap model Pro 100 oscillometric sphygmomanometer, Critikon, Tampa, Florida, USA).[21,23] Hypertension was defined as a systolic blood pressure ≥140 mmHg, a diastolic blood pressure ≥90 mmHg or use of antihypertension medication.[28] Diabetes mellitus was defined as a fasting blood glucose level ≥126 mg/dL or the use of diabetes mellitus medication; impaired fasting glucose was defined as a fasting glucose level of 100 to 125 mg/dL without use of diabetes mellitus medication.[27,28]

Laboratory Measurements

At Exam 1, blood samples were collected after a 12-hour fast and were analyzed in a central laboratory for glucose, total cholesterol, high-density lipoprotein cholesterol,

high-sensitivity C-reactive protein, interleukin-6, D-Dimer, and fibrinogen antigen.[21,23,29] The Modification of Diet in Renal Disease equation, indexing per 1.73 m^2 for body surface area was used to calculate the estimated glomerular filtration rate.[30] The central laboratory was responsible for training, certifying, and overseeing quality control of all Field Center laboratory technicians.[21]

CVD Event Adjudication

The MESA protocol for event adjudication has been reported previously.[21,31] CVD events examined were angina, definite and probable infarction, resuscitated cardiac arrest, CHD death, transient ischemic attack, stroke, and stroke death.[32] CHD events recorded were angina, myocardial infarction, resuscitated cardiac arrest, and CHD death.[32] Angina was defined as definite (evidence of CHD), probable (documentation of patient treatment for angina and ischemic symptoms) or absent. Stroke was defined as a neurologic event that lasted ≥24 hours or until death with a brain imaging finding.[32] Event data were collected through follow-up telephone calls, patient information at MESA visits, and medical records. Two independent physicians, masked to participant data, served as adjudicators.[31]

Carotid Ultrasound Imaging and IMT Measurement

The carotid imaging protocol for the MESA has been described previously.[28,33] Transverse and longitudinal images were acquired from the clavicle to the most distal portion of the internal carotid artery. Images were recorded on videotape using a GE 700 Logic ultrasound system and a M12L transducer (General Electric Medical Systems, Waukesha, WI, USA). Videotape images were digitized using the Medical Digital Recording device (PACSGEAR, Pleasanton, CA, USA) and converted to digital format (Digital Imaging and Communications in Medicine files).[28,33] Digital Imaging and Communications in Medicine images were imported into syngo Ultrasound Work Place reading stations at the University of Wisconsin Atherosclerosis Imaging Research Program MESA Carotid Ultrasound Reading Center. Arterial Health Package software (Siemens Medical, Malvern, PA, USA) was used to measure carotid IMT. Mean IMT of the distal 1.0 cm of the far walls of the right and left common carotid arteries (CCAs) were measured in triplicate and plaques were identified.[33]

Grayscale Analysis

Digital Imaging and Communications in Medicine files containing images of the distal CCAs at end-diastole were converted to bitmap images for grayscale analysis using LifeQ Medical Carotid Plaque Analysis Software (Nicosia, Cyprus) (see Data S1 for more detail on Grayscale Analysis Methods).[17] Grayscale texture features analyzed for this study were GSM, entropy, GLDS-C, and SGLDM-ASM. Grayscale analysis included normalization, standardization, segmentation, and feature extraction. Images were normalized such that the blackest area in the blood was assigned a grayscale value of 0 and the brightest white portion in the middle of the adventitia a grayscale value of 190. After normalization, images were standardized to a pixel density of 20/mm.[17,34] Segmentation of the arterial wall was performed by identifying the distal one centimeter (cm) segment of the CCA immediately proximal to the carotid bulb. The far wall of the distal CCA was segmented by tracing the blood-intima interface and media adventitia interface for a distance of 1 cm (Figure 1).[16,17] Grayscale texture features were extracted from the segmented wall using the LifeQ Medical software.

Grayscale Phantom Measurements

To determine the effect of acquisition from digitized videotape on grayscale features we performed a phantom study (experiment details and image provided in Data S1). We imaged a grayscale small parts phantom (404GS precision small parts grey scale phantom, Gammex Middleton, WI, USA) stored images directly (direct acquisition) from the Logic 700 system RGB video-out signal into the Medical Digital Recording device, and also recorded the same image with videotape first and then digitized the image (digitized from videotape) with the Medical Digital Recording device (Figure S1).

Feature Extraction

GSM and entropy are first-order statistics derived from the grayscale histogram.[35] GSM is the median grayscale value within the segmented region of interest of the arterial wall and represents echogenicity.[6,7,35] Entropy is a measure of randomness or uncertainty of how grayscale values are distributed in the image using the formula:[9,35]

$$ENT = -\sum_{i} p(i)\ \log(p(i))$$

where $p(i)$ is the probability that a grayscale value i is contained within the region of interest.[35]

GLDS methods use properties from the first-order statistics to measure the distribution of grayscale values and to assess the heterogeneity of region of interest. The measurement computes the differences in grayscale values between

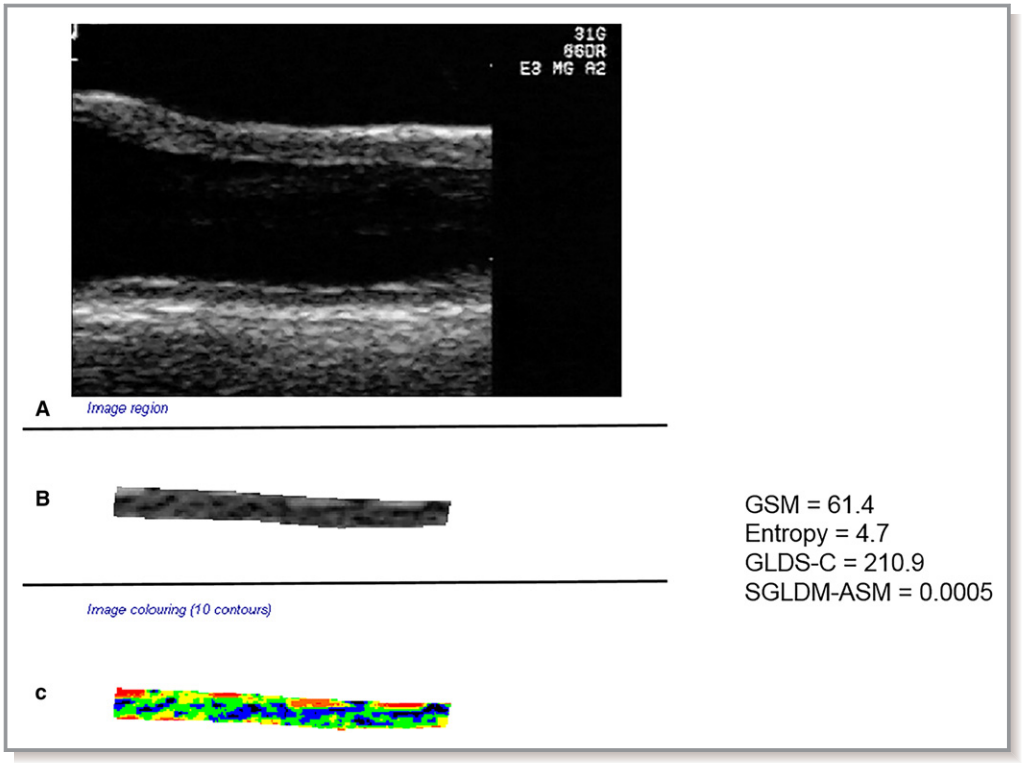

Figure 1. **A**, Demonstrates the B-mode grayscale image of the distal common carotid artery. **B**, Demonstrates the segmented grayscale distal 1.0 cm of the far wall of the common carotid artery. **C**, Demonstrates the colorized segmented distal common carotid artery. The LifeQ Medical software colorizes the pixels based on grayscale value, 0 to 25 black, 26 to 50 blue, 51 to 75 green, 76 to 100 yellow, 101 to 125 orange, 126 to 255 red.[36] The grayscale measures for this segmentation are GSM=61.4, entropy=4.7, GLDS-C=210.9 and SGLDM-ASM=0.0005.

pixels at different distances and directions using the formula:[6,7,35,36]

$$CON = \sum i^2 \; p_\delta(i)$$

where i is the difference between 2 pixels and $p_\delta(i)$ is the individual probabilities that a grayscale value will occur at a given distance.[35]

SGLDM methods characterize the texture of an image by calculating how often pairs of pixels with specific grayscale values occur next to each other at a specific distance and direction, with angles limited to 0, 45, 90, and 135 degrees. The SGLDM is constructed by calculating the frequency of each pair of pixels at a given distance and direction.[18] After construction of the SGLDM, ASM is computed using the following equation:[6,7,35]

$$f_1 = \sum_i \sum_j \{p(i,j)\}^2$$

where f_1 represents ASM, $p(i,j)$ is the $(i,j)^{th}$ element in the SGLDM matrix.[35]

Additional information about grayscale methods is provided in Figures S1 through S9.

Reproducibility

Two readers measured 22 carotid arterial wall images twice, masked to the first reading and to each other's measurements. The average (SD) GSM for reader 1 was 52.3 (24.7) units compared with 52.8 (26.7) units for reader 2. The first readings for each reader were used to examine inter-reader differences. The inter-observer absolute difference was 4.7 (5.0) units. The inter-observer within-subject standard deviation was 4.8 units and the intraclass correlation coefficient was 0.97 (95% CI 0.92 to 0.99). For GLDS-C the inter-observer within-subject standard deviation was 17.6 and the intraclass correlation coefficient was 0.91 (95% CI 0.80 to 0.96). Pearson correlation coefficients and linear regression are presented as a scattergram (GSM r=0.97, R^2=0.93; GLDS-C r=0.92, R^2=0.85) (Figure 2).

Statistical Analysis

We performed a case-cohort analysis that defined cases as participants who had any CVD event, as above. After excluding 29 participants who were ineligible for the MESA study or who had no follow-up data and excluding participants

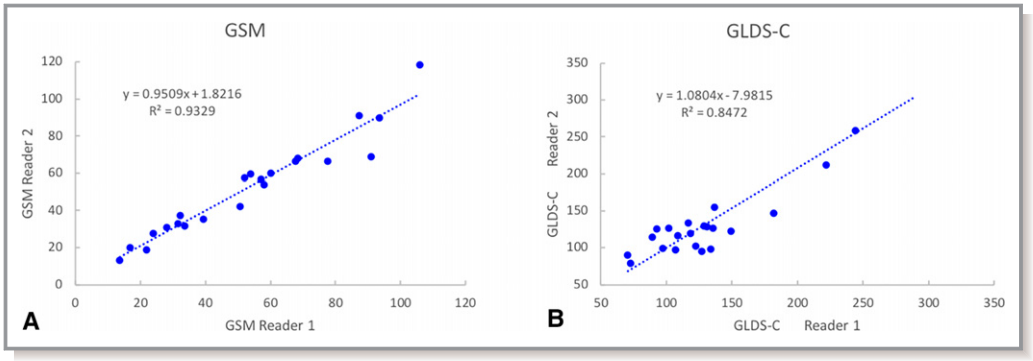

Figure 2. **A**, Inter-reader results for GSM measurements. **B**, Inter-reader results for GLDS-C. GSM indicates grayscale median; GLDS-C, gray level difference statistics-contrast.

at MESA sites with incompatible ultrasound grayscale maps, 491 participants were identified as cases. The subcohort was selected randomly from the 4651 participants who were eligible for inclusion. Because the subcohort is a random sample of the whole cohort, it included 94 incident cases, as shown in Figure 3.

R version 3.4.1 was used to perform all statistical analyses. Continuous variables are reported as means (SD). Categorical variables are reported as counts and percentages. SGLDM-ASM was natural log transformed. Multivariable linear regression models in the random subcohort were used to identify the strength and direction of associations between

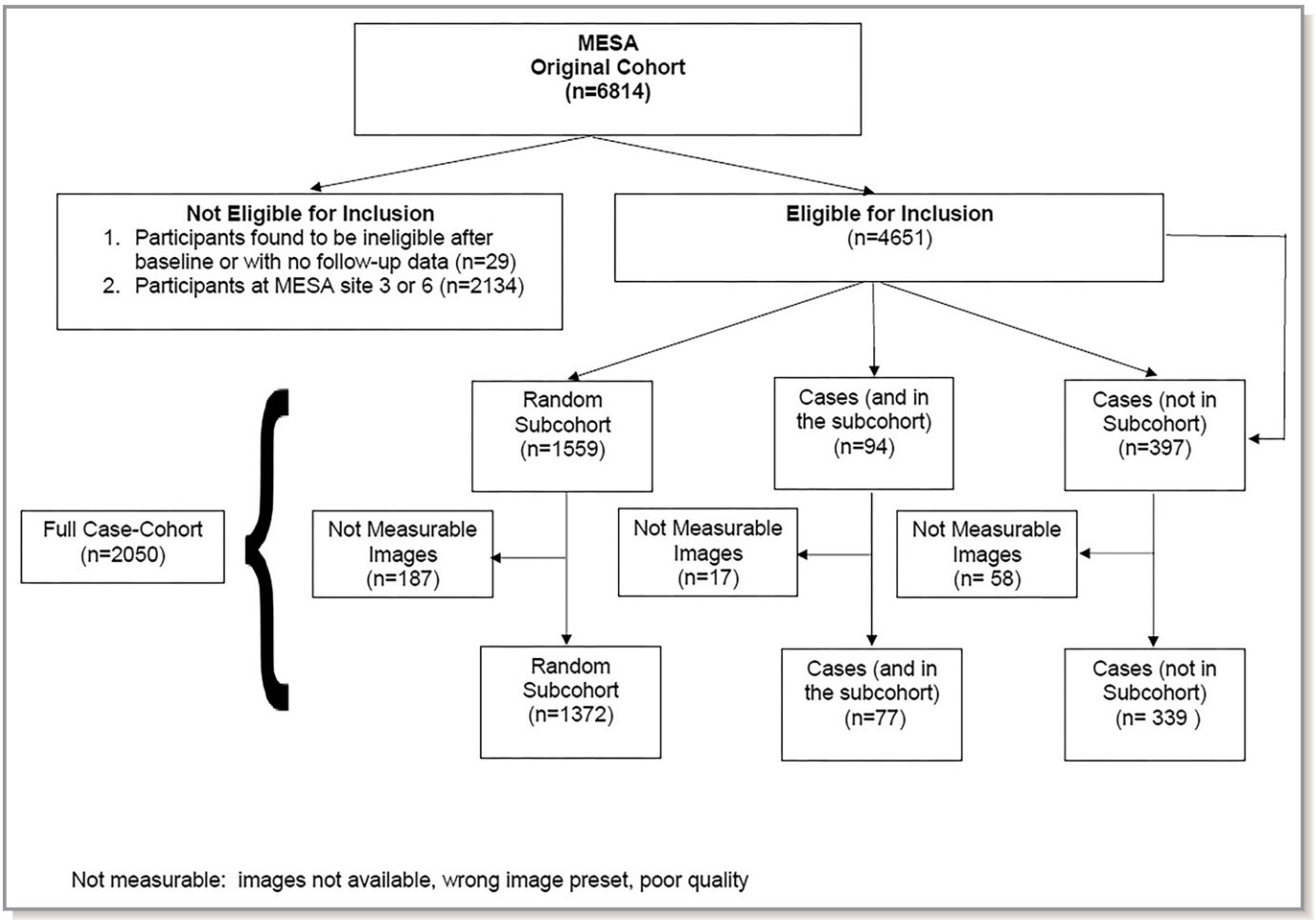

Figure 3. Case-Cohort Design, MESA sites 3 and 6 not included because of scanning with different imaging presets. MESA indicates Multi-Ethnic Study of Atherosclerosis.

each CVD risk factor and each ultrasound measure alone and after adjusting for age, sex, and race. All models used the minimum of the right and left CCA GSM, entropy, and GLDS-C values and the maximum of the right and left CCA SGLDM-ASM value. This represents the most severe side for each measurement and summarizes the data as a single observation per participant for each measure. Continuous variables are reported per SD increment. Cox proportional hazards models with inverse selection probability weighting were used to determine if standardized values for GSM, entropy, GLDS-C, and SGLDM-ASM could predict incident CHD, stroke, and CVD events over the follow-up period. Model 0 assessed associations between each image outcome and events without controlling for any other covariates. Model 1 assessed

Table 1. Participant Characteristics

	All (n=1788)	Non-Cases (n=1372)	Cases (n=416)
Age, y	63.1 (10.3)	61.84 (10.25)	67.42 (9.48)
Sex (n, %)			
Female	940 (52.6)	766 (55.8)	174 (41.8)
Male	848 (47.4)	606 (44.2)	242 (58.2)
Race (n, %)			
White	574 (32.1)	442 (32.2)	132 (31.7)
Black, African-American	497 (27.8)	379 (27.6)	118 (28.4)
Hispanic	416 (23.3)	308 (22.4)	108 (26)
Chinese-American	301 (16.8)	243 (17.7)	58 (13.9)
Smoking status (n, %)			
Never	931 (52.1)	748 (54.6)	183 (44)
Former	634 (35.5)	467 (34.1)	167 (40.1)
Current	221 (12.4)	155 (11.3)	66 (15.9)
Diabetes mellitus (n, %)			
Impaired fasting glucose	258 (14.5)	191 (14)	67 (16.1)
Normal	1275 (71.5)	1031 (75.4)	244 (58.8)
Diabetes mellitus	250 (14)	146 (10.7)	104 (25.1)
Hypertension (n, %)			
No	986 (55.1)	836 (60.9)	150 (36.1)
Yes	802 (44.9)	536 (39.1)	266 (63.9)
Systolic blood pressure (mmHg)	126.8 (21.7)	124.3 (20.9)	135.0 (22.4)
Diastolic blood pressure (mmHg)	72 (10.4)	71.3 (10.1)	74.3 (11.1)
Body-mass index (kg/m^2)	27.8 (5.3)	27.7 (5.4)	28 (5.1)
Total cholesterol (mmol/L)	5.1 (1.0)	5.1 (0.9)	5.1 (1.0)
High-density lipoprotein cholesterol (mmol/L)	1.4 (0.4)	1.4 (0.4)	1.3 (0.4)
C-reactive protein (nmol/L)	36.2 (63.8)	36.1 (65.1)	37.5 (58.5)
Interleukin-6 (pg/L)	1500 (1200)	1490 (1220)	1730 (1180)
D-Dimer (nmol/L)	2.2 (3.3)	1.9 (3.1)	2.3 (3.4)
Fibrinogen (μmol/L)	10.3 (2.2)	10.1 (2.2)	10.8 (2.4)
Carotid intima-media thickness (mm)	0.8 (0.2)	0.8 (0.2)	0.9 (0.2)
Carotid grayscale median (units)	61.9 (23.4)	62.7 (23.4)	59.1 (23.3)
Carotid entropy (units)	4.6 (0.2)	4.6 (0.2)	4.5 (0.2)
Carotid GLDS-C (units)	159.7 (70.3)	163.7 (71.8)	145.9 (62.8)
Carotid SGLD-ASM (log units)	−7.1 (0.7)	−7.1 (0.7)	−7.1 (0.8)

All values are mean (SD) unless noted otherwise. GLDS-C indicates gray level difference statistic-contrast; SGLDM-ASM, spatial gray level dependence matrices-angular second moment.

Table 2. Cross-Sectional Associations Between Imaging Markers and Cardiovascular Disease Risk Factors in the Random Subcohort (N=1449)

N=1449	Standard Deviation	Model 0 (Unadjusted)		Model 1 (Adjusted for Age, Sex, Race/Ethnicity)	
		β (95% CI)	*P* Value	β (95% CI)	*P* Value
Grayscale median					
Age, y	10.3	−2.94 (−3.99, −1.89)	<0.001*		
Sex (male)	-	0.62 (−1.51, 2.76)	0.567		
Race (Chinese-American)	-	14.69 (11.64, 17.74)	<0.001*		
Race (Black, African-American)	-	−0.01 (−2.65, 2.64)	0.997		
Race (Hispanic Latino)	-	2.45 (−0.36, 5.26)	0.088		
Body-mass index (kg/m^2)	5.4	−2.43 (−3.49, −1.38)	<0.001*	−1.06 (−2.16, 0.05)	0.061
Smoking status: Current		−3.75 (−7.18, −0.33)	0.032*	−2.28 (−5.66, 1.10)	0.185
Smoking status: Former	-	−2.26 (−4.57, 0.05)	0.055	0.57 (−1.76, 2.90)	0.633
Total cholesterol (mmol/L)	0.93	−0.89 (−1.95, 0.17)	0.100	−0.74 (−1.78, 0.30)	0.162
High-density lipoprotein cholesterol (mmol/L)	0.40	−1.13 (−2.19, −0.07)	0.037*	−0.35 (−1.48, 0.78)	0.543
Diabetes mellitus (IFG)	-	−2.03 (−5.10, 1.04)	0.195	−2.37 (−5.36, 0.62)	0.12
Diabetes mellitus (DM)	-	−1.43 (−4.84, 1.98)	0.410	−0.95 (−4.28, 2.38)	0.577
Hypertension (yes)	-	−4.47 (−6.62, −2.32)	<0.001*	−2.44 (−4.64, −0.24)	0.029*
C-reactive protein (nmol/L)	6381	−0.79 (−1.85, 0.28)	0.146	−0.19 (−1.22, 0.83)	0.711
Interleukin-6 (pg/L)	1200	−1.36 (−2.43, −0.29)	0.013*	−0.29 (−1.33, 0.76)	0.59
D-Dimer (nmol/L)	3.29	−1.69 (−2.75, −0.63)	0.002*	−0.72 (−1.76, 0.32)	0.175
Fibrinogen (μmol/L)	2.19	−1.88 (−2.94, −0.82)	0.001*	−0.99 (−2.05, 0.08)	0.070
Entropy					
Age, y	10.3	−0.03 (−0.04, −0.02)	<0.001*		
Sex (male)	-	0.00 (−0.02, 0.03)	0.794		
Race (Chinese-American)	-	0.02 (−0.02, 0.05)	0.357		
Race (Black, African-American)	-	0.01 (−0.02, 0.04)	0.455		
Race (Hispanic Latino)	-	0.00 (−0.03, 0.03)	0.989		
Body-mass index (kg/m^2)	5.4	0.00 (−0.01, 0.01)	0.865	−0.00 (−0.01, 0.01)	0.882
Smoking status: Current	-	−0.02 (−0.06, 0.02)	0.301	−0.03 (−0.07, 0.01)	0.102
Smoking status: Former	-	−0.01 (−0.04, 0.01)	0.266	−0.01 (−0.03, 0.02)	0.530
Total cholesterol (mmol/L)	0.93	−0.00 (−0.02, 0.01)	0.594	−0.00 (−0.01, 0.01)	0.821
High-density lipoprotein cholesterol (mmol/L)	0.40	−0.01 (−0.02, 0.00)	0.086	−0.01 (−0.02, 0.00)	0.19
Diabetes mellitus (IFG)	-	−0.02 (−0.05, 0.02)	0.290	−0.01 (−0.04, 0.02)	0.565
Diabetes mellitus (DM)	-	−0.01 (−0.04, 0.03)	0.693	0.00 (−0.04, 0.04)	0.896
Hypertension (yes)	-	−0.03 (−0.05, −0.00)	0.025*	−0.01 (−0.03, 0.02)	0.495
C-reactive protein (nmol/L)	6381	0.00 (−0.01, 0.01)	0.746	0.00 (−0.01, 0.01)	0.656
Interleukin-6 (pg/L)	1200	−0.00 (−0.02, 0.01)	0.473	0.00 (−0.01, 0.01)	0.949
D-Dimer (nmol/L)	3.29	−0.01 (−0.03, −0.00)	0.014*	−0.01 (−0.02, 0.00)	0.144
Fibrinogen (μmol/L)	2.19	−0.01 (−0.02, 0.00)	0.056	−0.01 (−0.02, 0.01)	0.263
GLDS-C					
Age, y	10.3	−14.4 (−17.17, −11.64)	<0.001*		
Sex (male)	-	−6.60 (−12.35, −0.85)	0.024*		
Race (Chinese-American)	-	−2.54 (−11.06, 5.97)	0.558		

Continued

Table 2. Continued

N=1449	Standard Deviation	Model 0 (Unadjusted)		Model 1 (Adjusted for Age, Sex, Race/Ethnicity)	
		β (95% CI)	*P* Value	β (95% CI)	*P* Value
Race (Black, African-American)	-	−5.33 (−12.73, 2.06)	0.157		
Race (Hispanic Latino)	-	−7.72 (−15.58, 0.13)	0.054		
Body-mass index (kg/m^2)	5.4	−5.36 (−8.21, −2.51)	<0.001*	−7.22 (−10.21, −4.23)	<0.001*
Smoking status: Current	-	−4.48 (−13.74, 4.79)	0.344	−7.87 (−17.07, 1.33)	0.093
Smoking status: Former	-	−5.40 (−11.65, 0.84)	0.090	−2.12 (−8.46, 4.22)	0.512
Total cholesterol (mmol/L)	0.93	−2.17 (−5.03, 0.69)	0.138	−2.34 (−5.16, 0.48)	0.104
High-density lipoprotein cholesterol (mmol/L)	0.40	2.62 (−0.24, 5.48)	0.072	2.77 (−0.31, 5.84)	0.078
Diabetes mellitus (IFG)	-	−10.12 (−18.35, −1.88)	0.016*	−4.13 (−12.25, 4.00)	0.319
Diabetes mellitus (DM)	-	−19.66 (−28.79, −10.53)	<0.001*	−12.47 (−21.52, −3.41)	0.007*
Hypertension (yes)	-	−16.55 (−22.32, −10.77)	<0.001*	−7.87 (−13.85, −1.89)	0.010*
C-reactive protein (nmol/L)	6381	−1.61 (−4.48, 1.25)	0.27	−1.49 (−4.29, 1.30)	0.295
Interleukin-6 (pg/L)	1200	−5.12 (−8.00, −2.24)	0.001*	−3.19 (−6.02, −0.36)	0.027*
D-Dimer (nmol/L)	3.29	−1.68 (−4.55, 1.19)	0.251	1.20 (−1.63, 4.03)	0.406
Fibrinogen (μmol/L)	2.19	−5.17 (−8.03, −2.32)	<0.001*	−3.40 (−6.30, −0.51)	0.021*
Log SGLDM-ASM					
Age, y	10.3	0.078 (0.04, 0.12)	<0.001*		
Sex (male)	-	−0.07 (−0.16, 0.01)	0.078		
Race (Chinese-American)	-	−0.25 (−0.37, −0.13)	<0.001*		
Race (Black, African-American)	-	0.04 (−0.06, 0.15)	0.427		
Race (Hispanic Latino)	-	−0.01 (−0.12, 0.10)	0.851		
Body-mass index (kg/m^2)	5.4	−0.01 (−0.05, 0.03)	0.538	−0.05 (−0.10, −0.01)	0.021*
Smoking status: Current	-	0.11 (−0.02, 0.24)	0.103	0.10 (−0.04, 0.24)	0.152
Smoking status: Former	-	0.03 (−0.06, 0.12)	0.578	−0.01 (−0.11, 0.08)	0.775
Total cholesterol (mmol/L)	0.93	0.01 (−0.04, 0.05)	0.758	−0.00 (−0.05, 0.04)	0.877
High-density lipoprotein cholesterol (mmol/L)	0.40	0.05 (0.01, 0.09)	0.021*	0.02 (−0.02, 0.07)	0.296
Diabetes mellitus (IFG)	-	−0.00 (−0.12, 0.12)	0.962	−0.00 (−0.12, 0.12)	0.99
Diabetes mellitus (DM)	-	−0.07 (−0.20, 0.06)	0.296	−0.10 (−0.23, 0.04)	0.152
Hypertension (yes)	-	0.09 (0.00, 0.17)	0.041*	0.03 (−0.06, 0.11)	0.583
C-reactive protein (nmol/L)	6381	0.01 (−0.03, 0.05)	0.571	−0.00 (−0.05, 0.04)	0.859
Interleukin-6 (pg/L)	1200	0.01 (−0.04, 0.05)	0.775	−0.02 (−0.06, 0.02)	0.380
D-Dimer (nmol/L)	3.29	0.08 (0.04, 0.12)	<0.001*	0.06 (0.02, 0.10)	0.006*
Fibrinogen (μmol/L)	2.19	0.04 (−0.01, 0.08)	0.096	0.01 (−0.04, 0.05)	0.768

Model 0 assessed unadjusted associations between each image outcome and each CVD risk factor; Model 1 assessed the same associations controlling for age, sex, and race. All continuous variables per SD increment. The SDs are calculated from the subcohort data. DM indicates diabetes mellitus; GLDS-C, gray level difference statistic-contrast; IFG, impaired fasting glucose; SGLDM-ASM, spatial gray level dependence matrices-angular second moment.
**P* value less than 0.05.

associations controlling for age, sex, and race/ethnicity. Model 2 examined associations as in model 1 with additional control for glycemic status (normal, impaired fasting glucose, diabetes mellitus), hypertension (yes/no), smoking status (never, former, current), total cholesterol, high-density lipoprotein cholesterol, body-mass index, and C-reactive protein. Model 3 examined associations as in model 2 with additional control for the mean of the right and left CCA IMT. These models described the ability of the grayscale measures to predict future CHD, stroke, and CVD events. Unadjusted Kaplan–Meier curves were used to examine tertile relationships of each grayscale marker to CHD, stroke and CVD

Table 3. Cox Proportional Hazard Models for Coronary Heart Disease

		Model 0 (Unadjusted)		Model 1 (Adjusted for Age, Sex, Race/Ethnicity)		Model 2 (Fully Adjusted)	
	Standard Deviation	Hazard Ratio (95% CI)	*P* Value	Hazard Ratio (95% CI)	*P* Value	Hazard Ratio (95% CI)	*P* Value
Grayscale median	20.6	0.84 (0.75, 0.95)	0.003*	0.92 (0.82, 1.03)	0.155	0.95 (0.84, 1.07)	0.361
Entropy	0.22	0.88 (0.79, 0.97)	0.014*	0.93 (0.84, 1.03)	0.142	0.90 (0.81, 1.00)	0.055
GLDS-C	54.6	0.69 (0.60, 0.79)	<0.001*	0.80 (0.70, 0.92)	0.001*	0.82 (0.71, 0.94)	0.005*
Log SGLDM-ASM	0.81	1.11 (1.01, 1.23)	0.039*	1.08 (0.97, 1.19)	0.154	1.11 (1.00, 1.23)	0.060

Fully adjusted model is adjusted for age, sex, race/ethnicity, glycemic status (normal, impaired fasting glucose, diabetes mellitus), hypertension (yes/no), smoking status (never, former, current), total cholesterol, high-density lipoprotein cholesterol, body-mass index, C-reactive protein. GLDS-C indicates gray level difference statistic-contrast; SGLDM-ASM, spatial gray level dependence matrices-angular second moment.
**P* value less than 0.05..

events. A sensitivity analysis was performed with additional adjustment for use of lipid-lowering medications.

Results

Participant Characteristics

At Exam 1, participants were mean (SD) 63.1 (10.3) years of age, 52.6% female, 32.1% white, 27.8% black, 23.3% Hispanic, and 16.8% Chinese (Table 1). Of the 2050 participants, 262 had images that were not measurable because they were not available, had poor image quality, or the ultrasonographer used an image optimization feature that changed the grayscale map, resulting in 1788 participants with at least 1 CCA image available. A total of 3106 images were analyzed from these participants. Grayscale values of CCA GSM, entropy, GLDS-C, SGLDM-ASM, carotid IMT, and CVD risk factors are presented in Table 1. There were 283 CHD, 120 stroke, and 416 CVD events over a median of 13 years follow-up.

Relationships Between Carotid Artery Grayscale Features and CVD Risk Factors

In unadjusted models, several statistically significant associations between CVD risk factors and GSM, entropy, GLDS-C, and SGLDM-ASM were identified (Table 2). After adjustment for age, sex, and race/ethnicity, we identified statistically significant inverse associations of GSM with hypertension, GLDS-C with body-mass index, diabetes mellitus, hypertension, interleukin-6, and fibrinogen, and SGLDM-ASM with body-mass index and D-Dimer. After adjustment for age, sex and race/ethnicity, entropy was not associated significantly with any CVD risk factor.

Grayscale Phantom Measurement Results

Grayscale texture feature measurements demonstrated small differences based on direct acquisition versus digitized from videotape (Data S1). Direct acquisition GSM 111.88, entropy 4.79, GLDS-C 255.26 and SGLDM-ASM 0.0002. Digitized from videotape GSM 103.38, entropy 4.76, GLDS-C 263.51, and SGLDM-ASM 0.0002 (Figure S1).

Cox Proportional Hazard Models

In unadjusted models, all 4 grayscale markers significantly predicted incident CHD and CVD events (Tables 3 through 5). Only GSM and GLDS-C predicted stroke events. When examining these markers by tertile, Kaplan–Meier curves demonstrated significant differences between the first and

Table 4. Cox Proportional Hazard Models for Stroke

		Model 0 (Unadjusted)		Model 1 (Adjusted for Age, Sex, Race/Ethnicity)		Model 2 (Fully Adjusted)	
	Standard Deviation	Hazard Ratio (95% CI)	*P* Value	Hazard Ratio (95% CI)	*P* Value	Hazard Ratio (95% CI)	*P* Value
Grayscale median	20.6	0.81 (0.68, 0.95)	0.012*	0.89 (0.75, 1.06)	0.196	0.91 (0.76 1.09)	0.306
Entropy	0.22	0.99 (0.83, 1.17)	0.873	1.06 (0.89, 1.25)	0.522	1.04 (0.87, 1.25)	0.636
GLDS-C	54.6	0.75 (0.62, 0.90)	0.002*	0.89 (0.74, 1.08)	0.249	0.96 (0.78, 1.17)	0.688
Log SGLDM-ASM	0.81	1.07 (0.91, 1.26)	0.434	1.01 (0.86, 1.18)	0.936	1.05 (0.89, 1.23)	0.582

Fully adjusted model is adjusted for age, sex, race/ethnicity, glycemic status (normal, impaired fasting glucose, diabetes mellitus), hypertension (yes/no), smoking status (never, former, current), total cholesterol, high-density lipoprotein cholesterol, body-mass index, C-reactive protein. GLDS-C indicates gray level difference statistic-contrast; SGLDM-ASM, spatial gray level dependence matrices-angular second moment.
**P* value less than 0.05.

Table 5. Cox Proportional Hazard Models for Cardiovascular Disease

		Model 0 (Unadjusted)		Model 1 (Adjusted for Age, Sex, Race/Ethnicity)		Model 2 (Fully Adjusted)	
	Standard Deviation	Hazard Ratio (95% CI)	*P* Value	Hazard Ratio (95% CI)	*P* Value	Hazard Ratio (95% CI)	*P* Value
Grayscale median	20.6	0.81 (0.74, 0.89)	<0.001*	0.89 (0.81, 0.98)	0.020*	0.92 (0.83,1.01)	0.084
Entropy	0.22	0.89 (0.82, 0.97)	0.006*	0.94 (0.87, 1.03)	0.187	0.93 (0.85, 1.01)	0.094
GLDS-C	54.6	0.70 (0.63, 0.78)	<0.001*	0.83 (0.74, 0.92)	0.001*	0.87 (0.77, 0.98)	0.018*
Log SGLDM-ASM	0.81	1.11 (1.02, 1.21)	0.016*	1.06 (0.98, 1.15)	0.165	1.09 (1.00, 1.19)	0.044*

Fully adjusted model is adjusted for age, sex, race/ethnicity, glycemic status (normal, impaired fasting glucose, diabetes mellitus), hypertension (yes/no), smoking status (never, former, current), total cholesterol, high-density lipoprotein cholesterol, body-mass index, C-reactive protein. GLDS-C indicates gray level difference statistic-contrast; SGLDM-ASM, spatial gray level dependence matrices-angular second moment.
**P* value less than 0.05.

third tertiles for GSM, entropy, and GLDS -C with risks for CHD and CVD (Figures 4 and 5). Kaplan–Meier curves also illustrated significant differences between the first and third tertiles for GSM and GLDS-C for stroke risk (Figure 6), and a lack of significant differences between the first and third tertile for SGLDM-ASM. In models adjusted for age, sex, and race/ethnicity, GSM predicted CVD events and GLDS-C predicted both CHD and CVD events. No grayscale markers were associated with stroke.

In models adjusted for age, sex, race/ethnicity, body-mass index, smoking status, total cholesterol, high-density lipoprotein-cholesterol, hypertension, diabetes mellitus, and C-reactive protein, GLDS-C independently predicted CHD and CVD events and SGLD-ASM independently predicted CVD events. No grayscale features independently predicted stroke. When carotid IMT was added to the models (data not shown), entropy, GLDS-C, and SGLDM-ASM, predicted CHD and CVD events and GSM predicted CVD events, but no grayscale markers were associated with stroke. We conducted a sensitivity analysis with additional adjustment for lipid lowering medications and results were not materially impacted.

Discussion

In this study, CCA grayscale texture features were associated with several CVD risk factors and predicted future adverse CVD events. These findings suggest that CVD risk factors, particularly serum lipid levels and markers of inflammation, influence the tissue structure and composition of the arterial wall and can be used to determine grayscale texture phenotypes associated with CVD risk.[1] Grayscale texture features may represent early changes in the arterial wall because of different environmental, genetic, and biological factors that initiate the atherosclerotic disease process.

Atherosclerosis is a multifactorial chronic systemic inflammatory disease that begins with injury to the endothelial cells lining the arterial wall.[37] Damage to the endothelial cells allows plasma low-density lipoprotein particles to cross the endothelium into the intimal layer resulting in inflammation, which recruits monocytes that transform into macrophages. Macrophages engulf the low-density lipoprotein particles forming arterial fatty streaks.[38] Vascular smooth muscle cells migrate from the media into the intima and initiate the formation of a fibrous cap over the fatty streak.[37] As the intima increases in size, the vasa vasorum proliferate.[39] As a consequence of these changes, the cellular content (ie, tissue components) of the arterial wall is altered.[37] Environmental exposure to CVD risk factors and epigenetic modifications contribute to disease progression and response to risk-reducing therapies.[40,41]

Grayscale texture features vary by tissue type as confirmed by comparing grayscale findings with carotid plaque histopathology examinations.[13,42] Plaque grayscale features associated with intra-operative visual assessment and histopathologic findings are; homogeneity (associated with more lipid content and inflammation),[15] low GSM (associated with higher lipid content, inflammation, increased macrophage concentration),[5,10,15,43] black areas near the surface of the plaque[44] (associated with ulceration),[13] and presence of discrete white areas (associated with increased inflammation and hemosiderin deposits).[13,34] Plaques with higher GSM have been associated with more calcium.[13,44] GSM increases in carotid plaques after 12 months of statin therapy;[45] CCA GSM also increases in individuals undergoing statin therapy,[46] demonstrating that grayscale markers reflect arterial wall cellular composition and can be used to monitor changes in the arterial wall associated with treatment.

In our study, the association of GSM with risk factors was not robust after adjustment for age, sex, and race/ethnicity; the only association we identified was with hypertension. Others have demonstrated associations between low GSM and increasing age, higher body-mass index, low levels of high-density lipoprotein cholesterol, high levels of low-density lipoprotein cholesterol, and circulating markers of inflammation and oxidative stress.[1–3,20] Those findings, however, were from smaller, more homogeneous cohorts often selected by

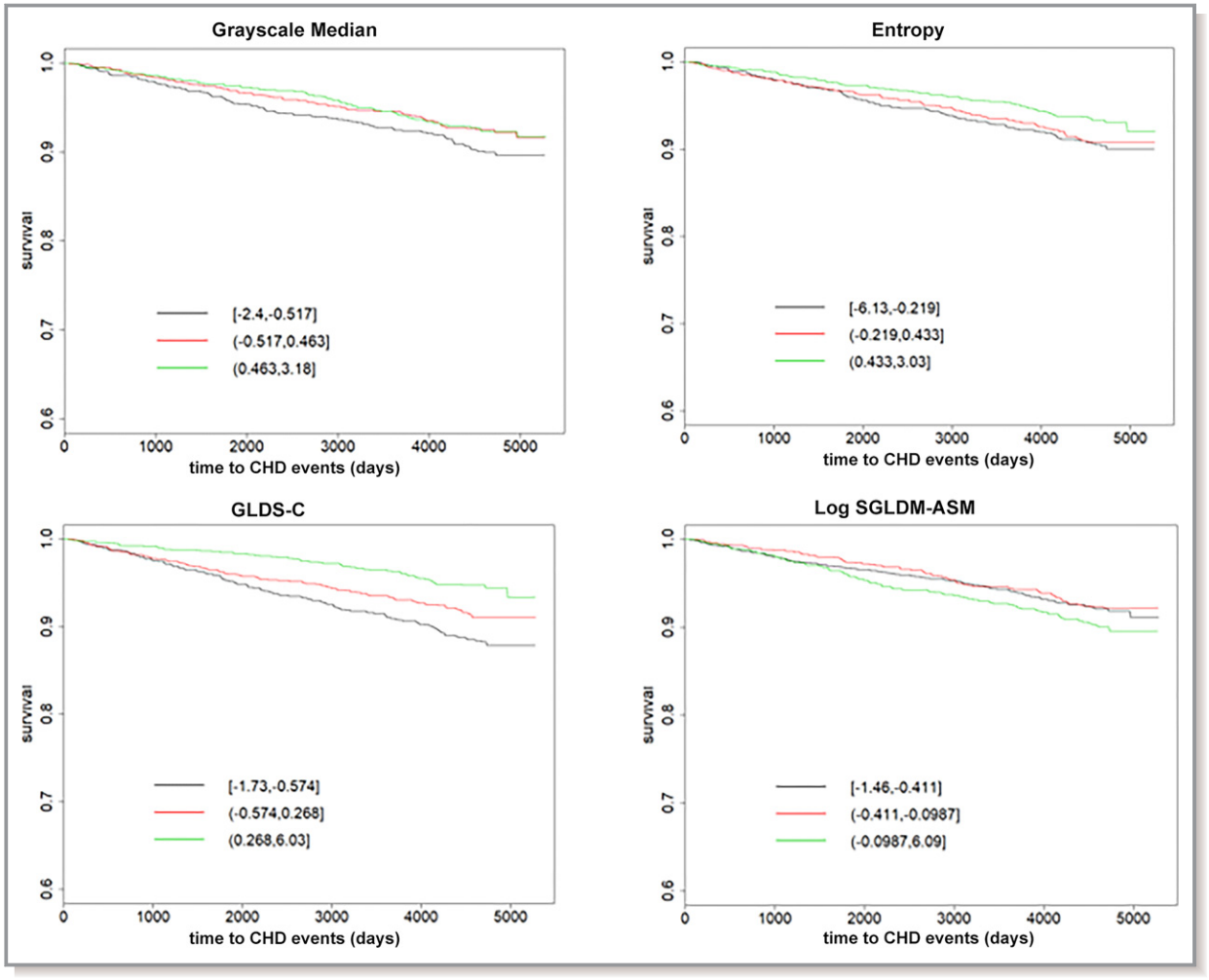

Figure 4. Kaplan–Meier Curves by tertile (coronary heart disease [CHD]). Black line is the lowest tertile/reference. Brackets display the range for each tertile of the standardized variable. Grayscale Median (Red: *P*=0.06, Green: *P*=0.04) (First tertile-black line [−2.4, −0.517], second tertile-red line [−0.517, 0.463], third tertile-green line [0.463, 3.18]), Entropy (Red: *P*=0.55, Green: *P*=0.02) (First tertile-black line [−6.13, −0.219], second tertile-red line [−0.219, 0.433), third tertile-green line [0.433, 3.03]), GLDS-C (Red: *P*=0.02, Green: *P*<0.001) (First tertile-black line [−1.73, −0.574], second tertile-red line [−0.574, 0.268], third tertile-green line [0.268, 6.03]) and SGLDM-ASM (Red: *P*=0.50, Green: *P*=0.10) (First tertile-black line [−1.46, −0.411], second tertile-red line [−0.411, −0.0987], third tertile-green line [−0.0987, 6.09]). GLDS-C indicates gray level difference statistics-contrast; SGLDM-ASM, spatial gray level dependence matrices-angular second moment.

age, sex, or disease status. MESA is, by definition, a multi-ethnic cohort composed of male and female participants aged 45 to 84 years free of known CVD at the time of enrollment. The other studies were performed in cohorts with participants aged ≥70 years of age,[2,3] women with human immunodeficiency virus,[20] or known risk factors for CVD.[1] Therefore, other studies may have imaged individuals that were further along in the atherosclerotic disease process so the overall measure of GSM, which reflects overall echogenicity, may best describe cellular content changes in the arterial wall. Our cohort was free of known CVD and therefore may be earlier in the atherosclerosis disease process, such that the overall measure of GSM cannot capture the early cellular composition changes, whereas the more sensitive measures of GLDS-C and SGLDM-ASM can identify differences in inter-pixel relationships by risk factor exposure.

In our study GLDS-C was associated with several CVD risk factors (ie, diabetes mellitus, hypertension, interleukin-6, and fibrinogen), even after adjusting for age, sex, and race/ethnicity. Changes in GLDS-C may represent one of the earliest changes associated with arterial injury, that of lipid and inflammatory cell infiltration into the arterial wall because it looks at inter-pixel relationships. We hypothesize that a healthy artery has a grayscale phenotype that results in different shades of gray in the wall reflecting greater differences in grayscale values between pixels. As lipids are deposited deep in the intimal layer and macrophages are recruited, the vessel wall becomes inflamed[47] and the normal

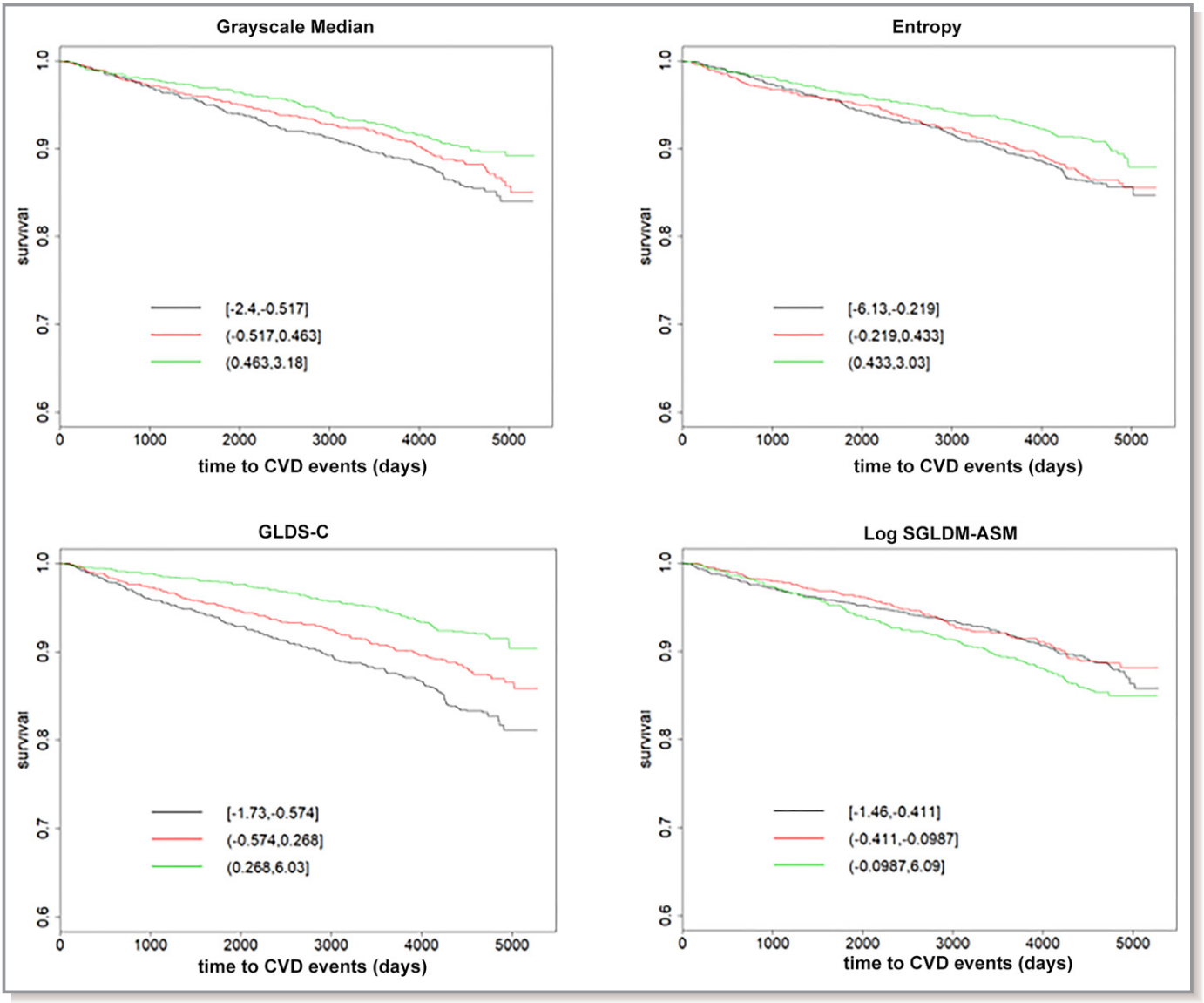

Figure 5. Kaplan–Meier Curves by tertile (Cardiovascular Disease [CVD]). Black line is the lowest tertile/reference. Brackets display the range for each tertile of the standardized variable. Grayscale Median (Red: P=0.17, Green: P<0.001) (First tertile-black line [−2.4, −0.517], second tertile-red line [−0.517, 0.463], third tertile-green line [0.463, 3.18]), Entropy (Red: P=0.71, Green: P=0.005) (First tertile-black line [−6.13, −0.219], second tertile-red line [−0.219, 0.433), third tertile-green line [0.433, 3.03]), GLDS-C (Red: P=0.002, Green: P<0.001) (First tertile-black line [−1.73, −0.574], second tertile-red line [−0.574, 0.268], third tertile-green line [0.268, 6.03]) and SGLDM-ASM (Red: P=0.35, Green: P=0.09) (First tertile-black line [−1.46, −0.411], second tertile-red line [−0.411, −0.0987], third tertile-green line [−0.0987, 6.09]). GLDS-C indicates gray level difference statistics-contrast; SGLDM-ASM, spatial gray level dependence matrices-angular second moment.

cellular structure is replaced by a grayscale phenotype with less variation in grayscale values (lower contrast). This hypothesis is supported in examining ultrasound images of arterial changes seen in patients with temporal arteritis, in which before treatment the walls are thick and hypoechoic and become thinner and more echogenic after effective treatment is established and the autoimmune inflammatory response is controlled.[48,49] These considerations also apply to SGLDM-ASM, which was independently associated with body-mass index and D-Dimer which also describes inter-pixel relationships, considering fixed distances apart.

Importantly, we also demonstrated, for the first time, that GLDS-C independently predicted future CHD and CVD events and that SGLDSM-ASM independently predicted future CVD events in this multi-ethnic cohort of middle-aged adults initially free of known CVD. These findings further suggest that grayscale markers that examine inter-pixel relationships may represent arterial injury could be used as biomarkers to assess risk for CVD. GSM was not a predictor of events in fully adjusted models in this study. As above, we hypothesize that GSM (a measure of overall echogenicity)[9] represents advanced arterial injury compared with GLDS-C and SGLDM-

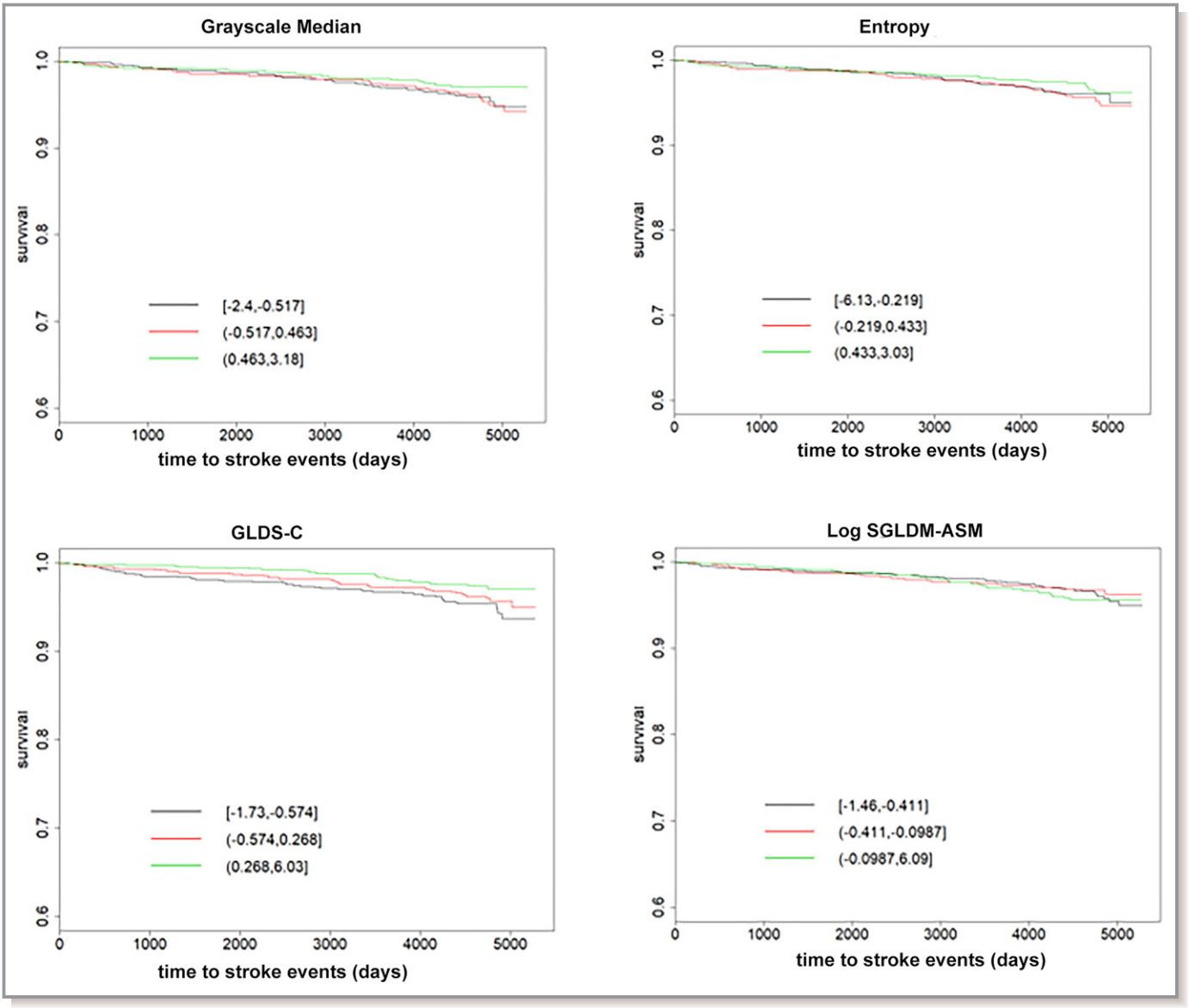

Figure 6. Kaplan–Meier Curves by tertile (Stroke). Black line is the lowest tertile/reference. Brackets display the range for each tertile of the standardized variable. Grayscale Median (Red: P=0.86, Green: P=0.04) (First tertile-black line [−2.4, −0.517], second tertile-red line [−0.517, 0.463], third tertile-green line [0.463, 3.18]), Entropy (Red: P=0.49, Green: P=0.33),(first tertile-black line [−6.13, −0.219], second tertile-red line [−0.219, 0.433], third tertile-green line [0.433, 3.03]), GLDS-C (Red: P=0.18, Green: P<0.001) (First tertile-black line [−1.73, −0.574], second tertile-red line [−0.574, 0.268], third tertile-green line [0.268, 6.03]) and SGLDM-ASM (Red: P=0.44, Green: P=0.82) (First tertile-black line [−1.46, −0.411], second tertile-red line [−0.411, −0.0987], third tertile-green line [−0.0987, 6.09]). GLDS-C indicates gray level difference statistics-contrast; SGLDM-ASM, spatial gray level dependence matrices-angular second moment.

ASM, which examine inter-pixel relationships,[9] and therefore may be better suited to examine subtle changes associated with early arterial injury and their ability to predict incident CHD and CVD events.

Limitations

The ultrasound technology used in this study no longer is state-of-the-art. Sonographers also were permitted to adjust overall image gain and time-gain-compensation settings. Ideally, the time-gain-compensation potentiometers would be set vertically through the vessel to standardize amplification of echoes through the near and far walls of the carotid artery.[34,50,51] Since this parameter was not standardized for image acquisition, differences between participants may have been affected unpredictably, though this would have created a null bias and decreased our ability to identify associations between our grayscale measures and CVD risk factors. It also would have been expected to attenuate CVD risk prediction. We did use a grayscale normalization process for all images to try to

overcome any effect that variation in time gain compensation settings may have had on the images. In addition to the older ultrasound technology, the ultrasound images were digitized from videotape for the grayscale analyses. We do not know what effect this may have had on our results, however, our phantom study demonstrated only small differences in grayscale measures and other studies have performed grayscale analysis on carotid plaque images digitized from videotape.[34,52] Future studies designed to examine grayscale texture features should include detailed instruction to standardize image acquisition,[34,50,51] instrumentation settings[53] and incorporate phantom studies to optimize extraction of grayscale texture features as described above.

Another limitation is that CVD risk-reducing therapies such as statins and hypertensive medications increased in use over time and may have altered the tissue composition in the arterial wall, though in a previous MESA analysis that accounted for time-varying use of risk-reducing therapies, association between risk factors and with carotid IMT and plaque progression were not notably affected.[33] Because we evaluated 4 imaging and 3 clinical end points, it is possible that some statistically significant associations may have been identified by chance.

We did not control for field center differences as these strongly reflect race differences in the MESA, so we controlled for race in our statistical models and not field center. Thus, any differences we see by race could in part be because of geographic or other differences between the sites.

Conclusions

Carotid artery grayscale texture features are associated with several CVD risk factors. Texture features that examine inter-pixel relationships independently predict CHD and CVD events. Our findings indicate that grayscale ultrasound features are novel imaging biomarkers that describe arterial wall structure, composition, and changes associated with early arterial injury and future CVD risk.

Acknowledgments

We thank JoAnne Weber, RDCS, RVT for measuring CCA grayscale features for this study. The authors thank the other investigators, the staff, and the participants of the MESA study for their valuable contributions. A full list of participating MESA investigators and institutions can be found at http://www.mesa-nhlbi.org.

Sources of Funding

This work was supported by an American Heart Association Midwest Grant-In-Aid 16GRNT29090009 and by contracts HHSN268201500003I, N01-HC-95159, N01-HC-95160, N01-HC-95161, N01-HC-95162, N01-HC-95163, N01-HC-95164, N01-HC-95165, N01-HC-95166, N01-HC-95167, N01-HC-95168, and N01-HC-95169 from the National Heart, Lung, and Blood Institute, and by grants UL1-TR-000040, UL1-TR-001079, and UL1-TR-001420 from National Center for Advancing Translational Sciences (NCATS). This publication also was developed under a Science to Achieve Results (STAR) research assistance agreement, No. RD831697 (MESA Air), awarded by the US Environmental Protection Agency. It has not been formally reviewed by the Environmental Protection Agency. The views expressed in this document are solely those of the authors and the Environmental Protection Agency does not endorse any products or commercial services mentioned in this publication.

Disclosures

Prof. Mitchell reports authorship contract with Davies Publishing, Inc, authorship with future royalties for textbook chapters with Elsevier and Wolters-Kluwer and contracted research grants from WL Gore to UW Madison. Dr Stein reports Wisconsin Alumni Research Foundation-patent related to carotid wall thickness and vascular age. The remaining authors have no disclosures to report.

References

1. Peters SA, Lind L, Palmer MK, Grobbee DE, Crouse JR III, O'Leary DH, Evans GW, Raichlen J, Bots ML, den Ruijter HM; METEOR study group. Increased age, high body mass index and low HDL-C levels are related to an echolucent carotid intima-media: the METEOR study. *J Intern Med*. 2012;272:257–266.
2. Wohlin M, Sundström J, Andrén B, Larsson A, Lind L. An echolucent carotid artery intima-media complex is a new and independent predictor of mortality in an elderly male cohort. *Atherosclerosis*. 2009;205:486–491.
3. Andersson J, Sundström J, Gustavsson T, Hulthe J, Elmgren A, Zilmer K, Zilmer M, Lind L. Echogenecity of the carotid intima-media complex is related to cardiovascular risk factors, dyslipidemia, oxidative stress and inflammation: the Prospective Investigation of the Vasculature in Uppsala Seniors (PIVUS) study. *Atherosclerosis*. 2009;204:612–618.
4. Lind L, Andersson J, Rönn M, Gustavsson T. The echogenecity of the intima-media complex in the common carotid artery is closely related to the echogenecity in plaques. *Atherosclerosis*. 2007;195:411–414.
5. Tegos TJ, Sohail M, Sabetai MM, Robless P, Akbar N, Pare G, Stansby G, Nicolaides AN. Echomorphologic and histopathologic characteristics of unstable carotid plaques. *AJNR Am J Neuroradiol*. 2000;21:1937–1944.
6. Kyriacou E, Pattichis MS, Christodoulou CI, Patichis CS, Kakkos S, Griffin M, Nicolaides A. Ultrasound imaging in the analysis of carotid plaque morphology for the assessment of stroke. In: Suri JS, Yuan C, Wilson DL, Laxminarayan S, eds. *Plaque Imaging: Pixel to Molecular Level. Stud Health Technol Inform*. IOS Press. 2005;113:241–275. Available at: http://ebooks.iospress.nl/publication/10191. Accessed September 6, 2018.
7. Christodoulou CI, Kyriacou E, Pattichis MS, Pattichis CS. Plaque feature extraction. In: Nicolaides A, Beach KW, Kyriacou E, Pattichis CS, eds. *Ultrasound and carotid bifurcation atherosclerosis*. London: Springer; 2012:223–246.
8. Stoitsis J, Golemati S, Nikita KS. A modular software system to assist interpretation of medical images—application to vascular ultrasound images. *IEEE Trans Instrum Meas*. 2006;55:1944–1952.
9. Griffin M, Kyriacou E, Kakkos SK, Beach KW, Nicolaides A. Image normalization, plaque typing, and texture feature extraction. In: Nicolaides A, Beach KW, Kyriacou E, Pattichis CS, eds. *Ultrasound and Carotid Bifurction Atherosclerosis*. London: Springer; 2012:193–211.

10. El-Barghouty NM, Levine T, Ladva S, Flanagan A, Nicolaides A. Histological verification of computerised carotid plaque characterisation. *Eur J Vasc Endovasc Surg*. 1996;11:414–416.
11. Loizou CP, Pantziaris M, Pattichis MS, Kyriacou E, Pattichis CS. Ultrasound image texture analysis of the intima and media layers of the common carotid artery and its correlation with age and gender. *Comput Med Imaging Graph*. 2009;33:317–324.
12. Loizou CP, Georgiou N, Griffin M, Kyriacou E, Nicolaides A, Pattichis CS. Texture analysis of the media-layer of the left and right common carotid artery. Paper presented at: IEEE-EMBS International Conference on Biomedical and Health Informatics (BHI). June 1-4, 2014; Valencia, Spain. https://ieeexplore-ieee-org.ezproxy.library.wisc.edu/abstract/document/6864456. Accessed December 31, 2018.
13. Mitchell CC, Stein JH, Cook TD, Salamat S, Wang X, Varghese T, Jackson DC, Sandoval Garcia C, Wilbrand SM, Dempsey RJ. Histopathologic validation of grayscale carotid plaque characteristics related to plaque vulnerability. *Ultrasound Med Biol*. 2017;43:129–137.
14. Salem MK, Bown MJ, Sayers RD, West K, Moore D, Nicolaides A, Robinson TG, Naylor AR. Identification of patients with a histologically unstable carotid plaque using ultrasonic plaque image analysis. *Eur J Vasc Endovasc Surg*. 2014;48:118–125.
15. Doonan RJ, Gorgui J, Veinot JP, Lai C, Kyriacou E, Corriveau MM, Steinmetz OK, Daskalopoulou SS. Plaque echodensity and textural features are associated with histologic carotid plaque instability. *J Vasc Surg*. 2016;64:671–677.e8.
16. Mitchell C, Piper ME, Korcarz CE, Hansen K, Weber J, Fiore MC, Baker TB, Stein JH. Echogenicity of the carotid arterial wall in active smokers. *J Diagn Med Sonogr*. 2018;34:161–168.
17. Mitchell CC, Korcarz CE, Tattersall MC, Gepner AD, Young RL, Post WS, Kaufman JD, McClelland RL, Stein JH. Carotid artery ultrasound texture, cardiovascular risk factors, and subclinical arterial disease: the Multi-Ethnic Study of Atherosclerosis (MESA). *Br J Radiol*. 2018;91:20170637.
18. Hall-Beyer M. GLCM Texture: A Tutorial v. 3.0 March 2017. Available at: https://prism.ucalgary.ca/handle/1880/51900/. Accessed September 6, 2018.
19. Bartolomucci F, Paterni M, Morizzo C, Kozakova M, D'Allitto N, Strippoli F, Palombo C, Maiorano G. Early structural changes of carotid artery in familial hypercholesterolemia. *Am J Hypertens*. 2001;14:125A–126A. Abstract.
20. Jung M, Parrinello CM, Xue X, Mack WJ, Anastos K, Lazar JM, Selzer RH, Shircore AM, Plankey M, Tien P, Cohen M, Gange SJ, Hodis HN, Kaplan RC. Echolucency of the carotid artery intima-media complex and intima-media thickness have different cardiovascular risk factor relationships: the Women's Interagency HIV Study. *J Am Heart Assoc*. 2015;4:pii: e001405. DOI: 10.1161/JAHA.114.001405.
21. Bild DE, Bluemke DA, Burke GL, Detrano R, Diez Roux AV, Folsom AR, Greenland P, Jacob DR Jr, Kronmal R, Liu K, Nelson JC, O'Leary D, Saad MF, Shea S, Szklo M, Tracy RP. Multi-Ethnic Study of Atherosclerosis: objectives and design. *Am J Epidemiol*. 2002;156:871–881.
22. National Institutes of Health, National Heart, Lung, and Blood Institute. Multi-Ethnic Study of Atherosclerosis (MESA). Biologic Specimen and Data Repository Information Coordinating Center. Website. https://biolincc.nhlbi.nih.gov/studies/mesa/?q=multi%20ethnic%20study%20of%20atherosclerosis. Last updated November 20, 2017. Accessed November 2, 2018.
23. Jain A, McClelland RL, Polak JF, Shea S, Burke GL, Bild DE, Watson KE, Budoff MJ, Liu K, Post WS, Folsom AR, Lima JA, Bluemke DA. Cardiovascular imaging for assessing cardiovascular risk in asymptomatic men versus women: the Multi-Ethnic Study of Atherosclerosis (MESA). *Circ Cardiovasc Imaging*. 2011;4:8–15.
24. Prentice RL. A case-cohort design for epidemiologic cohort studies and disease prevention trials. *Biometrika*. 1986;73:1–11.
25. Barlow WE, Ichikawa L, Rosner D, Izumi S. Analysis of case-cohort designs. *J Clin Epidemiol*. 1999;52:1165–1172.
26. Gregory JS. The application of the case-cohort method to data on pulp and paper mill workers in British Columbia. [Master of Science thesis]. Victoria, British Columbia, Canada: University of Victoria; 2001.
27. Mitchell C, Korcarz CE, Gepner AD, Kaufman JD, Post W, Tracy R, Gassett AJ, Ma N, McClelland RL, Stein JH. Ultrasound carotid plaque features, cardiovascular disease risk factors and events: the Multi-Ethnic Study of Atherosclerosis. *Atherosclerosis*. 2018;276:195–202.
28. Gepner AD, Colangelo LA, Reilly N, Korcarz CE, Kaufman JD, Stein JH. Carotid artery longitudinal displacement, cardiovascular disease and risk factors: the Multi-Ethnic Study of Atherosclerosis. *PLoS One*. 2015;10:e0142138.
29. Wasserman BA, Sharrett AR, Lai S, Gomes AS, Cushman M, Folsom AR, Bild DE, Kronmal RA, Sinha S, Bluemke DA. Risk factor associations with the presence of a lipid core in carotid plaque of asymptomatic individuals using high-resolution MRI: the Multi-Ethnic Study of Atherosclerosis (MESA). *Stroke*. 2008;39:329–335.
30. Geovanini GR, Wang R, Weng J, Tracy R, Jenny NS, Goldberger AL, Costa MD, Liu Y, Libby P, Redline S. Elevations in neutrophils with obstructive sleep apena: the Multi-Ethnic Study of Atherosclerosis (MESA). *Int J Cardiol*. 2018;257:318–323.
31. Tattersall MC, Guo M, Korcarz CE, Gepner AD, Kaufman JD, Liu KJ, Barr RG, Donohue KM, McClelland RL, Delaney JA, Stein JH. Asthma predicts cardiovascular disease events: the Multi-Ethnic Study of Atherosclerosis. *Arterioscler Thromb Vasc Biol*. 2015;35:1520–1525.
32. Gepner AD, Young R, Delaney JA, Budoff MJ, Polak JF, Blaha MJ, Post WS, Michos ED, Kaufman J, Stein JH. Comparison of carotid plaque score and coronary artery calcium score for predicting cardiovascular disease events: the Multi-Ethnic Study of Atherosclerosis. *J Am Heart Assoc*. 2017;6:e005179. DOI: 10.1161/JAHA.116.005179.
33. Tattersall MC, Gassett A, Korcarz CE, Gepner AD, Kaufman JD, Liu KJ, Astor BC, Sheppard L, Kronmal RA, Stein JH. Predictors of carotid thickness and plaque progression during a decade: the Multi-Ethnic Study of Atherosclerosis. *Stroke*. 2014;45:3257–3262.
34. Nicolaides AN, Kakkos SK, Kyriacou E, Griffin M, Sabetai M, Thomas DJ, Tegos T, Geroulakos G, Labropoulos N, Doré CJ, Morris TP, Naylor R, Abbott AL; Asymptomatic Carotid Stenosis and Risk of Stroke (ACSRS) Study Group. Asymptomatic internal carotid artery stenosis and cerebrovascular risk stratification. *J Vasc Surg*. 2010;52:1486–1496.e1–5.
35. LifeQMedical Version 4.5. Carotid Plaque Texture Analysis Research Software for Ultrasonic Arterial Wall and Atherosclerotic Plaques Measurements. Operation Manual Version 4.5. LifeQ Ltd, Cyprus 2013:1–45.
36. Skorton DJ, Collins SM, Nichols J, Pandian NG, Bean JA, Kerber RE. Quantitative texture analysis in two-dimensional echocardiography: application to the diagnosis of experimental myocardial contusion. *Circulation*. 1983;68:217–223.
37. Crowther MA. Pathogenesis of atherosclerosis. *Hematology Am Soc Hematol Educ Program*. 2005;2005:436–441.
38. Bartels ED, Christoffersen C, Lindholm MW, Nielsen LB. Altered metabolism of LDL in the arterial wall precedes atherosclerosis regression. *Circ Res*. 2015;117:933–942.
39. Geiringer E. Intimal vascularization and atherosclerosis. *J Pathol Bacteriol*. 1951;63:201–211.
40. Zhuang J, Luan P, Li H, Wang K, Zhang P, Xu YW, Peng W. The Yin-Yang dynamics of DNA methylation is the key regulator for smooth muscle cell phenotype switch and vascular remodeling. *Arterioscler Thromb Vasc Biol*. 2017;37:84–97.
41. Illi B, Ciarapica R, Capogrossi MC. Chromatin methylation and cardiovascular aging. *J Mol Cell Cardiol*. 2015;83:21–31.
42. Lal BK, Hobson RW II, Pappas PJ, Kubicka R, Hameed M, Chakhtoura EY, Jamil Z, Padberg FT Jr, Haser PB, Durán WN. Pixel distribution analysis of B-mode ultrasound scan images predicts histologic features of atherosclerotic carotid plaques. *J Vasc Surg*. 2002;35:1210–1217.
43. Grønholdt ML, Nordestgaard BG, Bentzon J, Wiebe BM, Zhou J, Falk E, Sillesen H. Macrophages are associated with lipid-rich carotid artery plaques, echolucency on B-mode imaging, and elevated plasma lipid levels. *J Vasc Surg*. 2002;35:137–145.
44. Sztajzel R, Momjian S, Momjian-Mayor I, Murith N, Djebaili K, Boissard G, Comelli M, Pizolatto G. Stratified gray-scale median analysis and color mapping of the carotid plaque: correlation with endarterectomy specimen histology of 28 patients. *Stroke*. 2005;36:741–745.
45. Kadoglou NP, Sailer N, Moumtzouoglou A, Kapelouzou A, Gerasimidis T, Liapis CD. Aggressive lipid-lowering is more effective than moderate lipid-lowering treatment in carotid plaque stabilization. *J Vasc Surg*. 2010;51:114–121.
46. Lind L, Peters SA, den Ruijter HM, Palmer MK, Grobbee DE, Crouse JR III, O'Leary DH, Evans GW, Raichlen JS, Bots ML; METEOR Study Group. Effect of rosuvastatin on the echolucency of the common carotid intima-media in low-risk individuals: the METEOR trial. *J Am Soc Echocardiogr*. 2012;25:1120–1127.e1.
47. Lusis AJ. Genetics of atherosclerosis. *Trends Genet*. 2012;28:267–275.
48. Romera-Villegas A, Vila-Coll R, Poca-Dias V, Cairols-Castellote MA. The role of color duplex sonography in the diagnosis of giant cell arteritis. *J Ultrasound Med*. 2004;23:1493–1498.
49. Schmidt WA, Kraft HE, Vorpahl K, Völker L, Gromnica-Ihle EJ. Color duplex ultrasonography in the diagnosis of temporal arteritis. *N Engl J Med*. 1997;337:1336–1342.
50. Griffin MB, Kyriacou E, Pattichis C, Bond D, Kakkos SK, Sabetai M, Geroulakos G, Georgiou N, Doré CJ, Nicolaides A. Juxtaluminal hypoechoic area in ultrasonic images of carotid plaques and hemispheric symptoms. *J Vasc Surg*. 2010;52:69–76.

51. Kakkos SK, Griffin MB, Nicolaides AN, Kyriacou E, Sabetai MM, Tegos T, Makris GC, Thomas DJ, Geroulakos G; Asymptomatic Carotid Stenosis and Risk of Stroke (ACSRS) Study Group. The size of juxtaluminal hypoechoic area in ultrasound images of asymptomatic carotid plaques predicts the occurrence of stroke. *J Vasc Surg*. 2013;57:609–618.e1; discussion 617–618.

52. Ibrahimi P, Jashari F, Johansson E, Gronlund C, Bajraktari G, Wester P, Henein MY. Vulnerable plaques in the contralateral carotid arteries in symptomatic patients: a detailed ultrasound analysis. *Atherosclerosis*. 2014;235:526–531.

53. Steffel CN, Brown R, Korcarz CE, Varghese T, Stein JH, Wilbrand SM, Dempsey RJ, Mitchell CC. Influence of ultrasound system and gain on grayscale median values. *J Ultrasound Med*. 2018. Available at: doi: htpps://doi.org/10.1002/jum.14690. Accessed January 12, 2019.

SUPPLEMENTAL MATERIAL

Data S1.

Supplemental Methods

Grayscale analysis

We and others have previously reported methods for normalizing, standardizing and extracting texture features from ultrasound images.[1-8] This appendix provides additional information for these methods as used in this study.

Carotid ultrasound images were recorded on Super (s)-VHS video tapes using the GE 700 Logic ultrasound system and M12L transducer (General Electric Medical Systems, Waukesha, WI, USA). Video tape images were digitized using the NAI Tech Products Medical Digital Recording device (PACSGEAR, Pleasanton, CA, USA) and converted to digital format (Digital Imaging and Communications in Medicine files, DICOM).[9, 10] To examine how the videotape digitizing process may affect grayscale texture measurements we imaged a grayscale small parts phantom (404GS precision small parts grey scale phantom, Gammex Middleton, WI, USA) stored images directly from the Logic 700 system RGB video-out signal into the Medical Digital Recording device, and also recorded the same image with videotape first and then digitized the image with the Medical Digital Recording device (Figure S1).

DICOM files containing images of the distal CCAs at end-diastole were converted to bitmap images for grayscale analysis using LifeQ Medical Plaque Analysis Software (Nicosia, Cyprus).[7] Bitmap images were then normalized so that the blackest part of the blood was assigned a grayscale value of 0 and the brightest white part of the adventitia was assigned a grayscale value of 190 (Figures S2-S4).

After normalization, the images were standardized to a pixel density of 20 pixels per millimeter (Figure S5).

The far wall of the distal one centimeter of the CCA was segmented by tracing the blood-intima interface and media adventitia interface for a length of one centimeter (Figure S6).[7, 8] Grayscale texture features were extracted from the segmented wall using the LifeQ Medical software.

Texture Features

Texture features extracted for this study were the first order statistics grayscale median (GSM) and entropy. The gray level difference statistic method was used to extract the texture feature contrast (GLDS-CON) and the spatial gray level dependence matrices (SGLDM) method was used to measure angular second moment (SGLDM-ASM) (Figure S7).

These four texture features can be used to describe and quantitate grayscale properties of an image (Figure S8).

In images of the carotid arterial wall grayscale patterns also can be demonstrated (Figure S9). Images with similar overall echogenicity described by the GSM measurement can have very different measures of entropy, GLDS-CON and SGLDM-ASM. GLDS-CON and SGLDM-ASM examine inter-pixel relationships.

In this work, GLDS-CON and SGLDM-ASM were associated with several CVD risk factors and CVD events. Thus, we and others believe that these measures of inter-pixel relationships may represent early cellular changes in the arterial wall associated with injury and changes in tissue composition.

Figure S1. Measurement of grayscale median (GSM), entropy, gray level difference statistic-contrast (GLDS-CON) and spatial gray level dependence matrices-angular second moment (SGLDM-ASM).

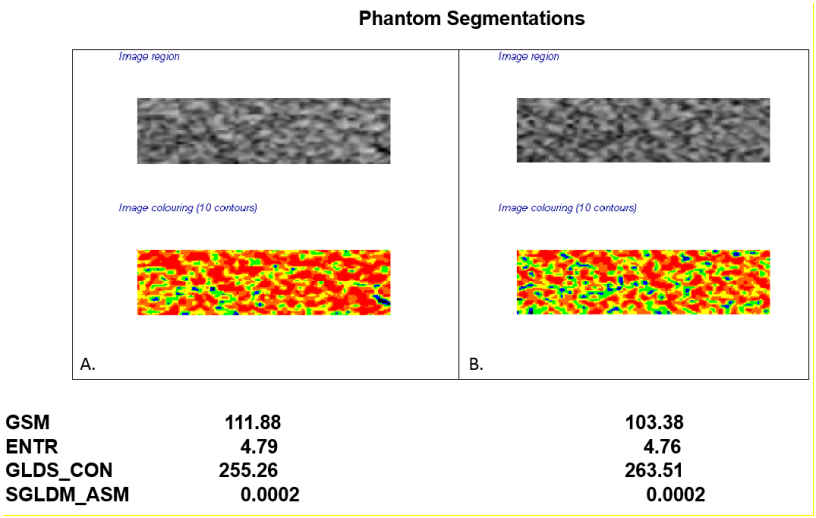

Panel A phantom segmentation of images derived directly from the system. Panel B segmentation performed from digitized-videotaped images.

Figure S2. Normalization process using the LifeQ Plaque Analysis software on a carotid artery image.

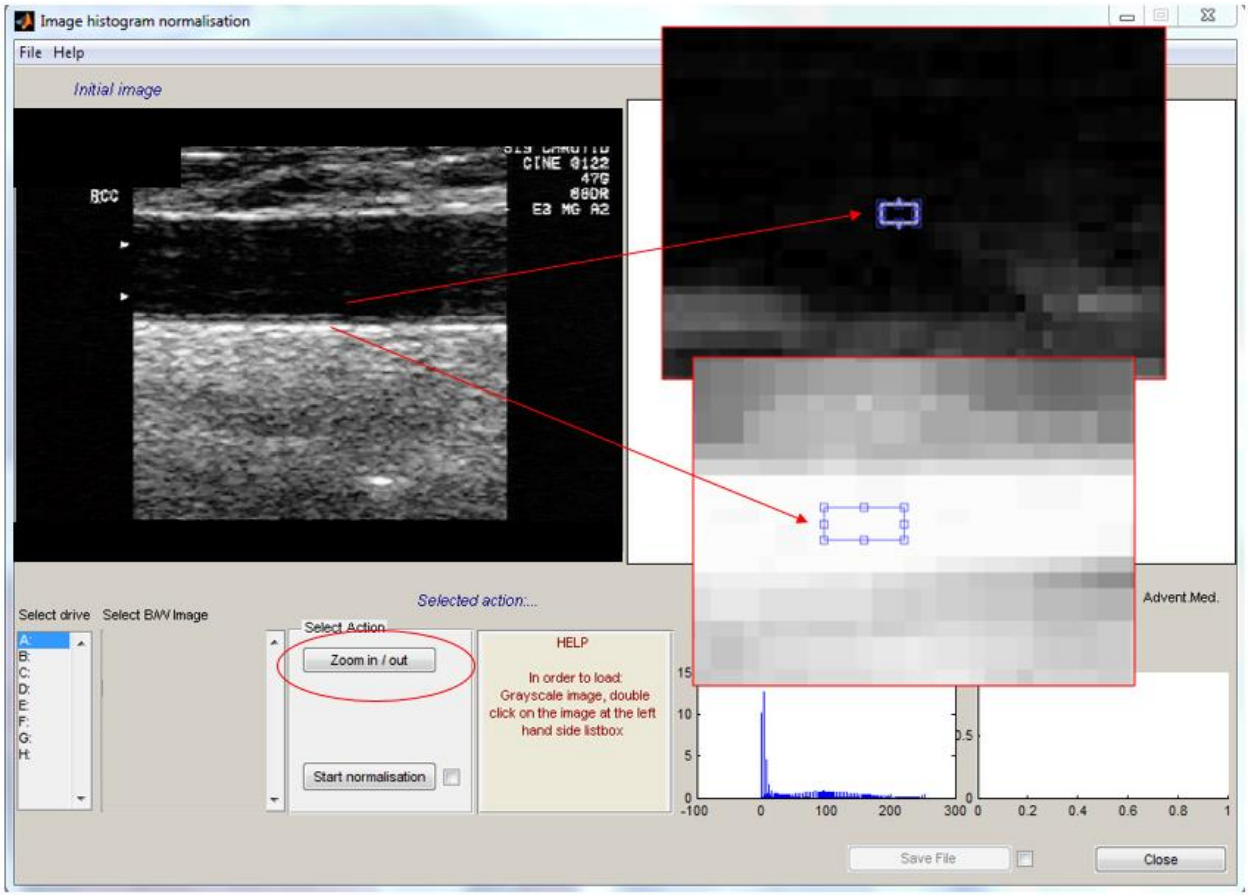

The blackest area of the blood is zoomed and a region of interest identified. This is entered as the blood and assigned a grayscale value of 0. The brightest white area of the adventitia is then identified, zoomed and the middle two-fourths identified. This area is then assigned a grayscale value of 190.

Figure S3. This figure demonstrates a pattern in which there are only two shades of gray depicted (gray shade = black or gray shade = white).

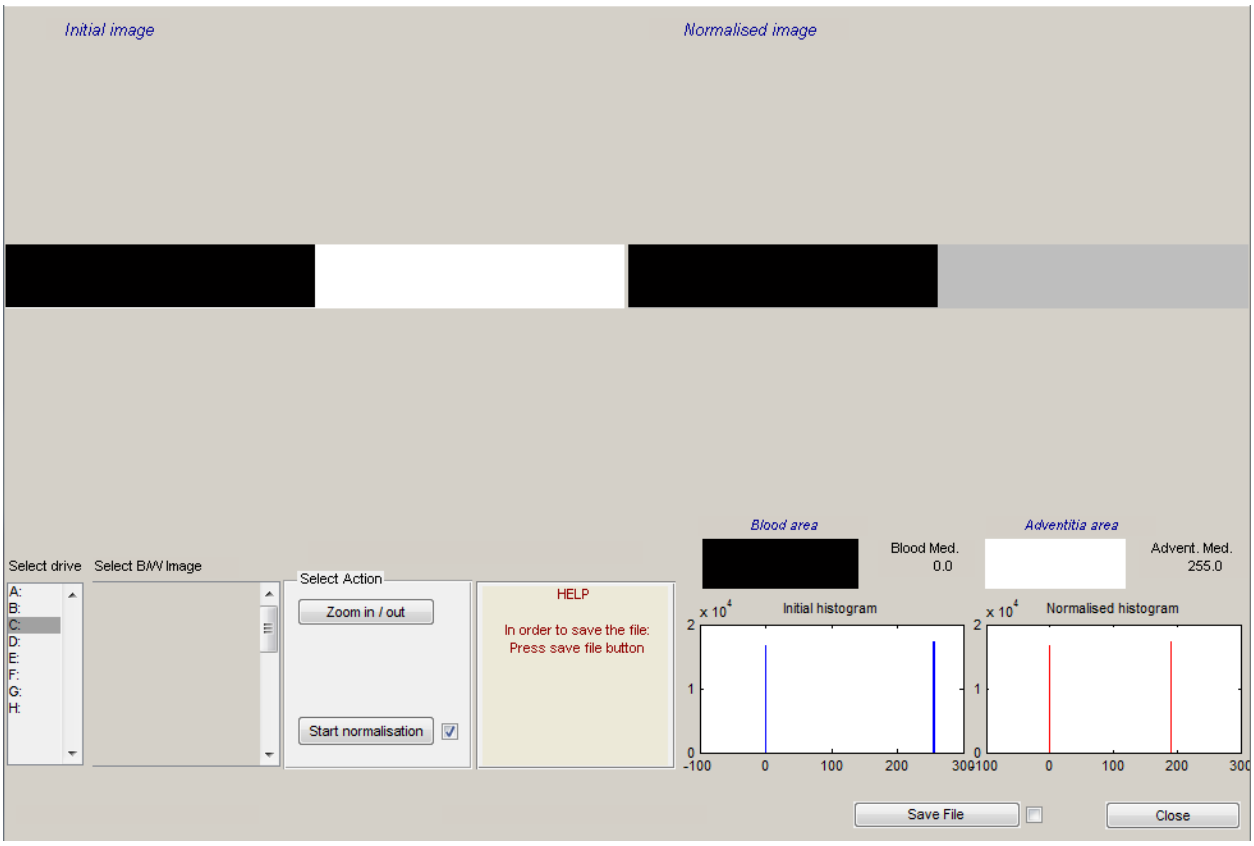

Note that on the initial image the black area has a grayscale value of 0 and the white area has a grayscale value of 255 (initial histogram). After normalization the grayscale values have been linearly scaled to the two reference points. Note the white area now appears gray on the normalized image and the normalized histogram demonstrates grayscale values of 0 and 190.

Figure S4. Example of common carotid artery initial image histogram, and then the normalized image loaded in the LifeQ Plaque Analysis software.

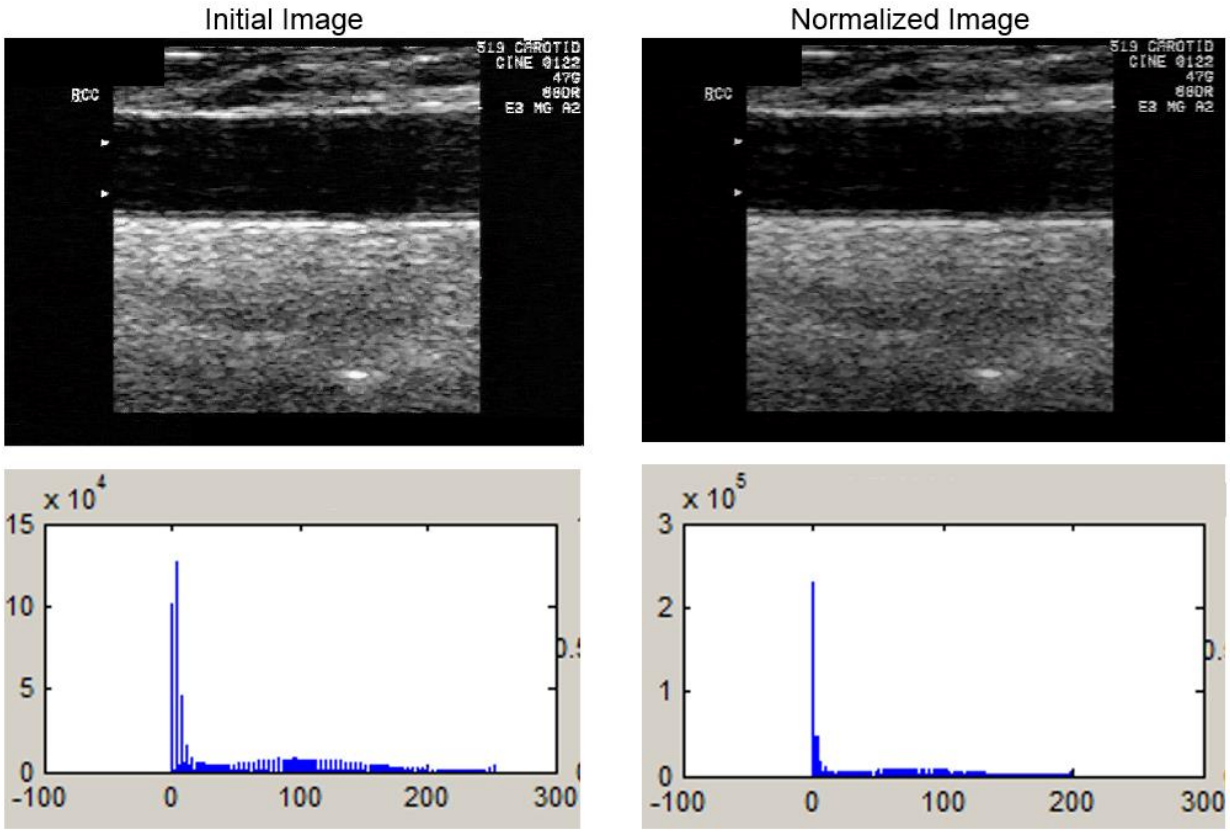

Note the initial image histogram (left panel) demonstrates grayscale values near 250 and after the image is normalized (right panel) the grayscale values are less than 200.

Figure S5. Example of initial image resolution 25.2 pixels per millimeter.

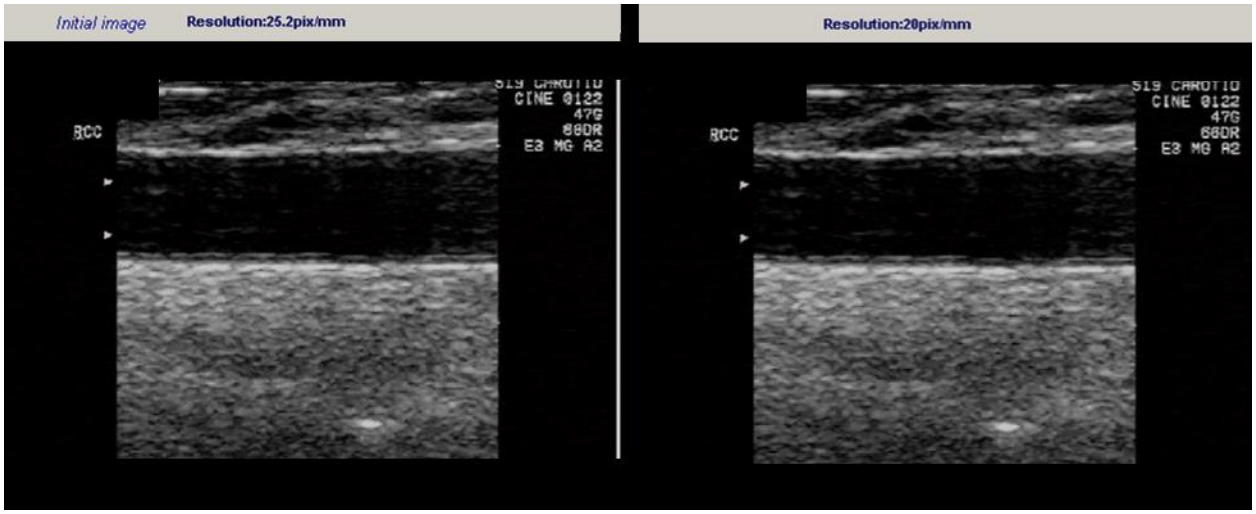

After standardization pixel density is 20 pixels per millimeter.

Figure S6. Example of how the distal one centimeter of the far wall of the common carotid artery was identified for segmentation.

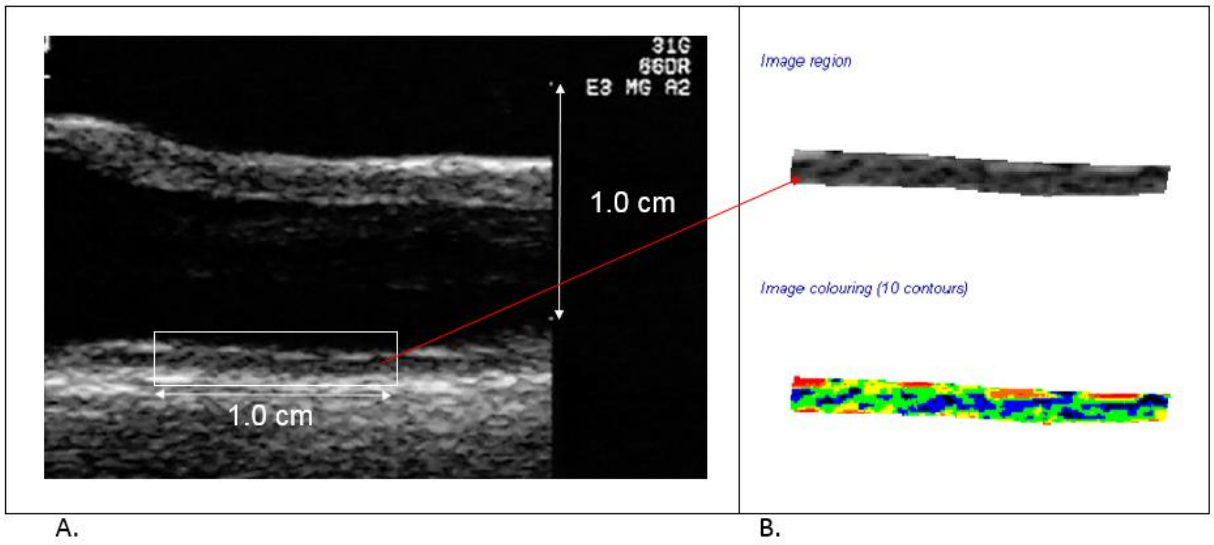

Panel A, one centimeter was identified using the markers on the side of the image. The white rectangle identifies the segment of the artery where the software would then be used to manually trace the region of interest. Panel B demonstrates the segmented arterial wall in grayscale and then colorized with the software based on the grayscale value.

Figure S7. Example of the extracted texture features using the LifeQ Medical Plaque Analysis software.

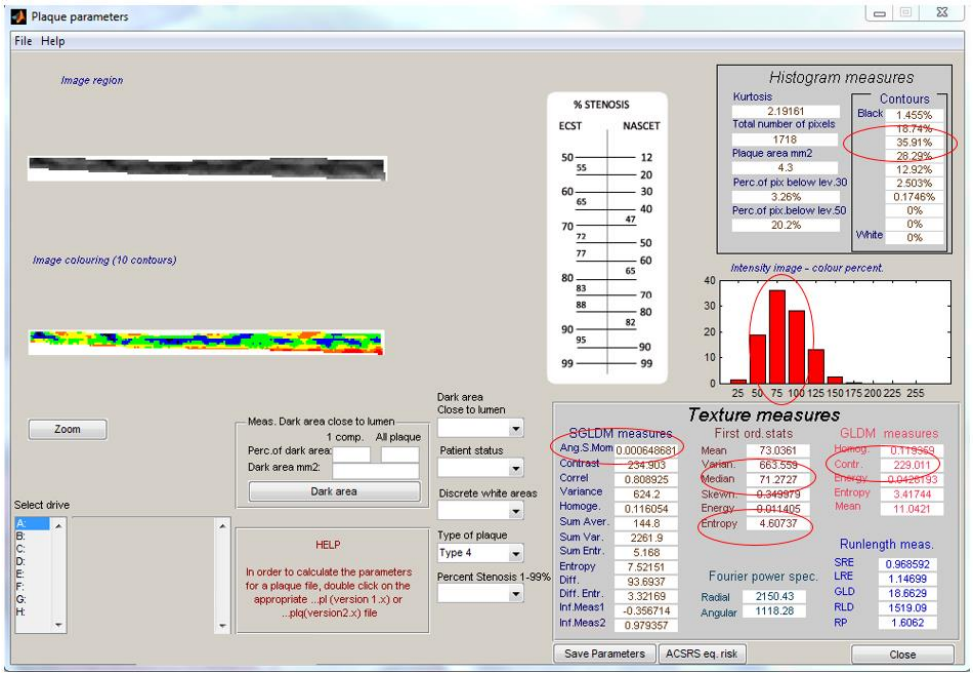

The first order statistics (First ord. stats, grayscale median [Median] value is 71.2727, entropy is 4.60737) are derived from the image histogram (Intensity image-color percent). The gray level difference statistic method (GLDM measures) for calculating contrast is 229.011. The spatial gray level dependence matrices (SGLDM) for calculating angular second moment (Ang. S. Mom is 0.000648681). The grayscale values are colorized with this software as follows; 0-25 = black, 26-50 = blue, 51-75=green, 76-100=yellow, 101-125= orange, 126-255=red.[11]

Figure S8. Grayscale measurements of grayscale median (GSM), entropy, gray level difference statistics – contrast (GLDS-CON) and spatial gray level dependence matrices – angular second moment (SGLDM-ASM) from square patterns.

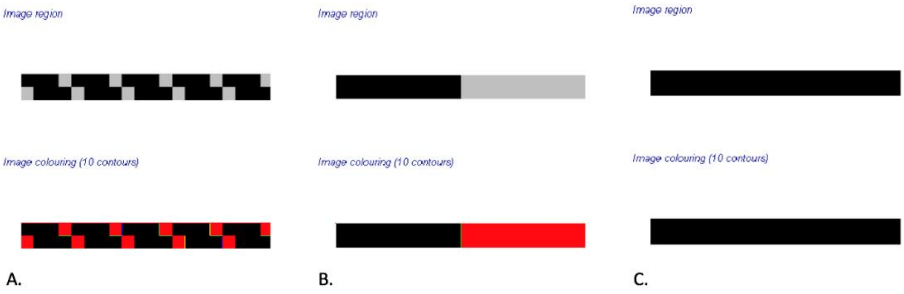

GSM	**0.00**	**0.00**	**0.00**
Entropy	**1.08**	**0.72**	**0.00**
GLDS-CON	**878.60**	**41.66**	**0.00**
SGLDM-ASM	**0.52**	**0.49**	**1.00**

Note that panels A,B and C all have a grayscale median value of 0.00, however, they have very different values for entropy, GLDS-CON and SGLDM-ASM demonstrating how these measures can further describe grayscale patterns.

Figure S9. Grayscale measurements of grayscale median (GSM), entropy, gray level difference statistics – contrast (GLDS-CON) and spatial gray level dependence matrices – angular second moment (SGLDM-ASM) from two different study participants (panel A and panel B).

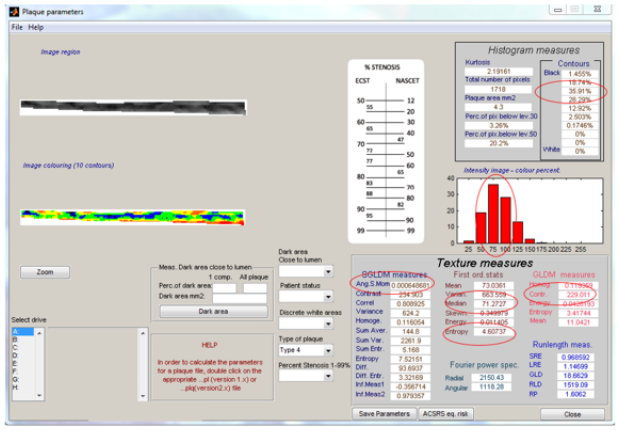

A.

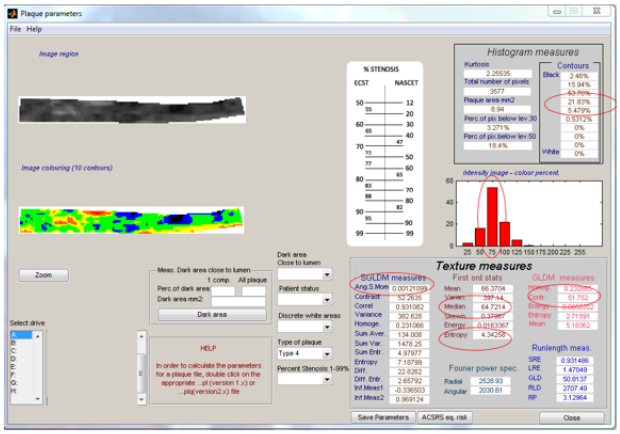

B.

GSM	**71.2727**	**64.7214**
Entropy	**4.60737**	**4.34258**
GLDS-CON	**229.011**	**51.752**
SGLDM-ASM	**0.000648681**	**0.00121099**

Note that the grayscale median value is not that different (71.2727 and 64.7214), however, they have very different values for the gray level difference statistics method contrast (GLDS-CON) and the spatial gray level dependence matrices – angular second motion (SGLDM-ASM) values demonstrating how these measures can further describe grayscale patterns by examining inter-pixel relationships.

Supplemental References:

1. Nicolaides AN, Kakkos SK, Kyriacou E, Griffin M, Sabetai M, Thomas DJ, Tegos T, Geroulakos G, Labropoulos N, Doré CJ, Morris TP, Naylor R, Abbott AL. Asymptomatic Carotid Stenosis and Risk of Stroke (ACSRS) Study Group. Asymptomatic internal carotid artery stenosis and cerebrovascular risk stratification. *J Vasc Surg*. 2010;52:1486-96 e1-5.

2. Griffin M, Nicolaides A, Kyriacou E. Normalisation of ultrasonic images of atherosclerotic plaques and reproducibility of grey scale median using dedicated software. *Int Angiol*. 2007;26:372-7.

3. Griffin MB, Kyriacou E, Pattichis C, Bond D, Kakkos SK, Sabetai M, Geroulakos G, Georgiou N, Doré CJ, Nicolaides A. Juxtaluminal hypoechoic area in ultrasonic images of carotid plaques and hemispheric symptoms. *J Vasc Surg*. 2010;52:69-76.

4. Griffin M, Kyriacou E, Kakkos SK, Beach KW, Nicolaides A. Image normalization, plaque typing, and texture feature extraction. In: A. Nicolaides, K. W. Beach, E. Kyriacou and C. S. Pattichis, eds. *Ultrasound and Carotid Bifurcation Atherosclerosis.* London: Springer; 2012:193-211.

5. Salem MK, Bown MJ, Sayers RD, West K, Moore D, Nicolaides A, Robinson TG, Naylor AR. Identification of patients with a histologically unstable carotid plaque using ultrasonic plaque image analysis. *Eur J Vasc Endovasc Surg*. 2014;48:118-25.

6. Doonan RJ, Gorgui J, Veinot JP, Lai C, Kyriacou E, Corriveau MM, Steinmetz OK, Daskalopoulou SS. Plaque echodensity and textural features are associated with histologic carotid plaque instability. *J Vasc Surg*. 2016;64:671-677 e8.

7. Mitchell CC, Korcarz CE, Tattersall MC, Gepner AD, Young RL, Post WS, Kaufman JD, McClelland RL, Stein JH. Carotid artery ultrasound texture, cardiovascular risk factors, and subclinical arterial disease: the Multi-Ethnic Study of Atherosclerosis (MESA). *Br J Radiol*. 2018;91:20170637.

8. Mitchell C, Piper ME, Korcarz CE, Hansen K, Weber J, Fiore MC, Baker TB, Stein JH. Echogenicity of the carotid arterial wall in active smokers. *J Diagn Med Sonogr*. 2018;34:161-168.

9. Gepner AD, Colangelo LA, Reilly N, Korcarz CE, Kaufman JD, Stein JH. Carotid artery longitudinal displacement, cardiovascular disease and risk factors: The Multi-Ethnic Study of Atherosclerosis. *PLoS One*. 2015;10:e0142138.

10. Tattersall MC, Gassett A, Korcarz CE, Gepner AD, Kaufman JD, Liu KJ, Astor BC, Sheppard L, Kronmal RA, Stein JH. Predictors of carotid thickness and plaque progression during a decade: the Multi-Ethnic Study of Atherosclerosis. *Stroke*. 2014;45:3257-62.

11. LifeQMedical Version 4.5. Carotid Plaque Texture Analysis Research Software for Ultrasonic Arterial Wall and Atherosclerotic Plaques Measurements. Operation Manual Version 4.5. LifeQ Ltd, Cyprus 2013:1-45.